



Applied
Remote Sensing
and Analysis

September 30, 2013



Juneau LiDAR and Orthophotos

Technical Data Report – Final Delivery



Bruce Simonson
City and Borough of Juneau
155 South Seward Street
Juneau, AK 99801
PH: 907.586.0754



WSI Corvallis Office
517 SW 2nd St., Suite 400
Corvallis, OR 97333
PH: 541-752-1204

TABLE OF CONTENTS

- INTRODUCTION 3
- ACQUISITION 6
 - PLANNING 6
 - GROUND SURVEY..... 7
 - MONUMENTATION..... 7
 - RTK SURVEYS 8
 - AERIAL TARGETS 9
 - LAND COVER 10
 - AIRBORNE SURVEY 12
 - LIDAR..... 12
 - DIGITAL IMAGERY..... 13
- PROCESSING 14
 - LIDAR DATA..... 14
 - INTENSITY NORMALIZATION..... 17
 - FEATURE EXTRACTION 18
 - CONTOURS..... 18
 - HYDRO-FLATTENING 19
 - DIGITAL IMAGERY 20
- RESULTS & DISCUSSION..... 21
 - LIDAR DENSITY 21
 - LIDAR ACCURACY ASSESSMENTS..... 26
 - LIDAR ABSOLUTE ACCURACY 26
 - LIDAR RELATIVE ACCURACY..... 28
 - DIGITAL IMAGERY ACCURACY ASSESSMENT 30
- SELECTED IMAGES..... 34
- CERTIFICATIONS 38
- APPENDIX A – MLLW ADJUSTMENT 41
- APPENDIX B - GLOSSARY..... 42
- APPENDIX C - ACCURACY CONTROLS..... 44

Cover Photo: View looking down the Mendenhall Glacier. Image created from gridded LiDAR points colored by 15-cm 4-band orthoimagery (left) and NIR imagery (right).

INTRODUCTION

View of survey equipment set up in the Juneau project area showing both tidal and mountainous terrain in the distance.



In April 2013, WSI (Watershed Sciences, Inc.) was contracted by the City and Borough of Juneau (CBJ) to collect Light Detection and Ranging (LiDAR) data and digital imagery in the spring of 2013 for the Juneau site in Alaska. Data were collected to aid CBJ in assessing the topographic and geophysical properties of the study area to support municipal planning, habitat assessments, and general development in the region.

This report accompanies the delivered LiDAR data and imagery for the entire survey site and documents data acquisition procedures, processing methods, and results of all accuracy assessments. Project specifics are shown in Table 1, the project extent can be seen in Figure 1, and a complete list of contracted deliverables provided to CBJ can be found in Table 2.

Table 1: Acquisition dates, acreages, and data types collected for the Juneau Area

Project Site	Contracted Acres	Contracted Acres	Acquisition Dates	Data Type
Juneau Site	109,978	121,313	5/8-9/2013 5/16/2013 5/20-23/2013 5/25-27/2013 5/29/2013 6/2-3/2013 6/11/2013	LiDAR
			5/28-29/2013 6/3/2013 6/11/2013	4 band (RGB/NIR) Digital Imagery

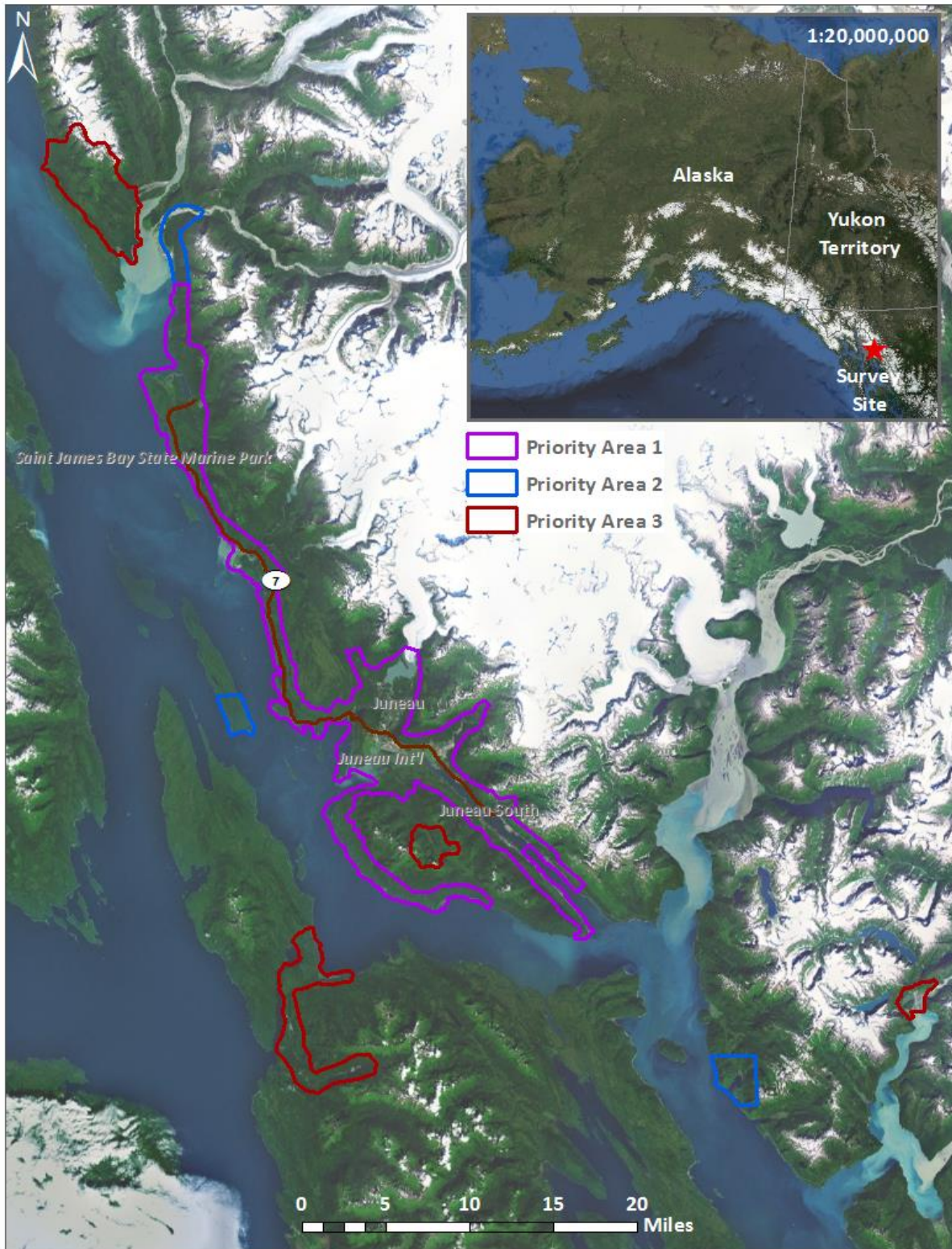


Figure 1: Location map of the Juneau site in Southeast Alaska

Table 2: Products delivered to CBJ for the Juneau area. The LAS point cloud is being delivered in 3 separate projections as per CBJ request.

Juneau Products		
Projection: UTM Zone 8 North Horizontal Datum: NAD83 2011 Vertical Datum: NAVD88 (GEOID12a) Units: Meters	Projection: Alaska State Plane Zone 1 Horizontal Datum: NAD83 2011 Vertical Datum: NAVD88 (GEOID12a) Units: US Survey Feet	Projection: Geographic Horizontal Datum: WGS84 (G1674) Vertical Datum: Ellipsoid Units: Decimal Degrees, Meters (LAS files only)
<i>All geoid and ellipsoid heights adjusted to Mean Lower Low Water</i>		
LAS Files	LAS v 1.2 and ASCII <ul style="list-style-type: none"> All Returns Ground Returns 	
Rasters	1-meter/3-foot ESRI Grids <ul style="list-style-type: none"> Bare Earth Model Hydroflattened Bare Earth Model Highest Hit Model Canopy Height Model TINs 0.5-meter/1.5-foot GeoTiffs <ul style="list-style-type: none"> Normalized Intensity Images 	
Vectors	Shapefiles (*.shp) <ul style="list-style-type: none"> Site Boundary LiDAR Index DEM/DSM Index Hydrolines (water's edge and shoreline) Bridge Footprints Contours (1-ft, 0.5-m) Base Stations, RTK, and Land Cover RTK Smooth Best Estimate Trajectory (SBETs) Point Void Polygons 	
Digital Imagery	Orthoimagery Index (*.shp) Photo Block Files Image Center Point (*.shp) Rasters: 15-centimeter pixel size (Priority 1) <ul style="list-style-type: none"> 4-band Orthorectified Imagery Mosaics (GeoTIFF and JPG2000) 4-band Unrectified frames (TIFF) Rasters: 30-centimeter pixel size (Priority 2&3) <ul style="list-style-type: none"> 4-band Orthorectified Imagery Mosaics (GeoTIFF and JPG2000) 4-band Unrectified frames (TIFF) 	

WSI Cessna Caravan



Planning

In preparation for data collection, WSI reviewed the project area using Google Earth, and flightlines were developed using a combination of specialized software. Careful planning by acquisition staff entailed adapting the pulse rate, flight altitude, scan angle, and ground speed to ensure complete coverage of the survey sites at the target point density of ≥ 4 and ≥ 8 pulses per square meter (0.74 pulses/square foot). Efforts are taken to optimize flight paths by minimizing flight times while meeting all accuracy specifications.

Factors such as satellite constellation availability and weather windows must be considered during the planning stage. Any weather hazards or conditions affecting the flight were continuously monitored due to their potential impact on the daily success of airborne and ground operations. In addition, a variety of logistical considerations required review including snow coverage, tidal conditions, site access, potential air space restrictions, and availability of company resources (both staff and equipment).

LiDAR acquisition of near shore areas was prioritized to coincide with the lowest tides possible, within constraints of daily local weather patterns. Leaf-off, no snow conditions were targeted in all other areas given the diverse terrain represented in the study area. Orthophoto collection occurred during similar tidal windows with the additional constraints of cloud and sun angle conditions.

Ground Survey

Ground survey data are used to geospatially correct the aircraft positional coordinate data and to perform quality assurance checks on final LiDAR data and orthoimagery products. Ground surveys, including monumentation and ground check points, are conducted to support the airborne acquisition process.



Monumentation

The spatial configuration of ground survey monuments provided redundant control for LiDAR flights. Due to limited road access within the study area, baseline lengths were extended to cover outlying areas of interest. Priority 1 was held to $\leq 13\text{nm}$ radius, Priority 2 was held to $\leq 16\text{nm}$ radius and Priority 3 did not exceed 21nm . Monuments were also used for collection of ground control points using RTK survey techniques (see RTK below).

Monument locations were selected with consideration for satellite visibility, field crew safety, and optimal location for RTK coverage. WSI established 5 new monuments and utilized 4 existing monuments for the Juneau project (Table 3, Figure 2). New monumentation was set using $5/8'' \times 30''$ rebar topped with stamped 2" aluminum caps. R&M Engineering, Inc. (Mark A. Johnson - AKPLS#7570) certified all monuments and performed the Mean Lower Low Water (MLLW) adjustment. See *Certifications* and *Appendix A* at the end of this report for more information on the MLLW adjustment.

Table 3: Monuments established for the Juneau acquisition. Coordinates are on the NAD83 (2011) datum, epoch 2010.00. "Ellipsoid MLLW" elevations have been adjusted to the Mean Lower Low Water datum established by the NOAA and AK DOT adjustment of 2011.

Monument ID	Type	Latitude	Longitude	Ellipsoid (meters)	Ellipsoid MLLW (m)
AI4907	Existing NGS	58° 21' 25.76343"	134° 35' 48.94834"	8.632	9.703
AI4908	Existing NGS	58° 17' 56.74744"	134° 25' 09.76530"	9.680	10.811
GPS_11	Existing WSI	58° 39' 00.30674"	134° 55' 16.72403"	17.091	18.070
JUNEAU_01	New WSI	58° 23' 05.66089"	134° 44' 35.95245"	38.490	39.538
JUNEAU_02	New WSI	58° 21' 10.20746"	134° 30' 41.40839"	8.631	9.718
JUNEAU_03	New WSI	58° 15' 34.87988"	134° 19' 28.18192"	8.317	9.378
JUNEAU_04	New WSI	58° 31' 15.29855"	134° 47' 30.08158"	11.327	12.301
JUNEAU_05	New WSI	58° 16' 38.12145"	134° 30' 58.90446"	346.298	347.410
TONGASS_01	Existing WSI	58° 36' 45.74532"	134° 55' 54.44028"	36.180	37.120

To correct the continuous onboard measurements of the aircraft position recorded throughout the missions, WSI concurrently conducted multiple static Global Navigation Satellite System (GNSS) ground surveys (1 Hz recording frequency) over each monument. After the airborne survey, the static GPS data were triangulated with nearby Continuously Operating Reference Stations (CORS) using the Online Positioning User Service (OPUS¹) for precise positioning. Multiple independent sessions over the same monument were processed to confirm antenna height measurements and to refine position accuracy.

RTK Surveys

For the real time kinematic (RTK) check point data collection, a Trimble R7 base unit was positioned at a nearby monument to broadcast a kinematic correction to a roving Trimble R8 GNSS receiver. All RTK measurements were made during periods with a Position Dilution of Precision (PDOP) of ≤ 3.0 with at least six satellites in view of the stationary and roving receivers. When collecting RTK data, the rover would record data while stationary for five seconds, then calculate the pseudorange position using at least three one-second epochs. Relative errors for the position must be less than 1.5 cm horizontal and 2.0 cm vertical in order to be accepted. See Table 4 for Trimble unit specifications.

RTK positions were collected on paved roads and other hard surface locations such as gravel or stable dirt roads that also had good satellite visibility. RTK measurements were not taken on highly reflective surfaces such as center line stripes or lane markings on roads due to the increased noise seen in the laser returns over these surfaces. The distribution of RTK points depended on ground access constraints and may not be equitably distributed throughout the study area. See Figure 2 for the distribution of RTK in this project.

Table 4: Trimble equipment identification

Receiver Model	Antenna	Example	OPUS Antenna ID	Use
Trimble R7 GNSS	Zephyr GNSS Geodetic Model 2 RoHS		TRM57971.00	Static
Trimble R8	Integrated Antenna R8 Model 2		TRM_R8_GNSS	Static, RTK

¹ OPUS is a free service provided by the National Geodetic Survey to process corrected monument positions. <http://www.ngs.noaa.gov/OPUS>.

Aerial Targets

Aerial targets were placed throughout the project area prior to imagery acquisition in order to geospatially correct the orthoimagery. Located within RTK range of the ground survey monuments, the targets were secured with surveyor's nails and routinely checked for disturbance (Figure 2).

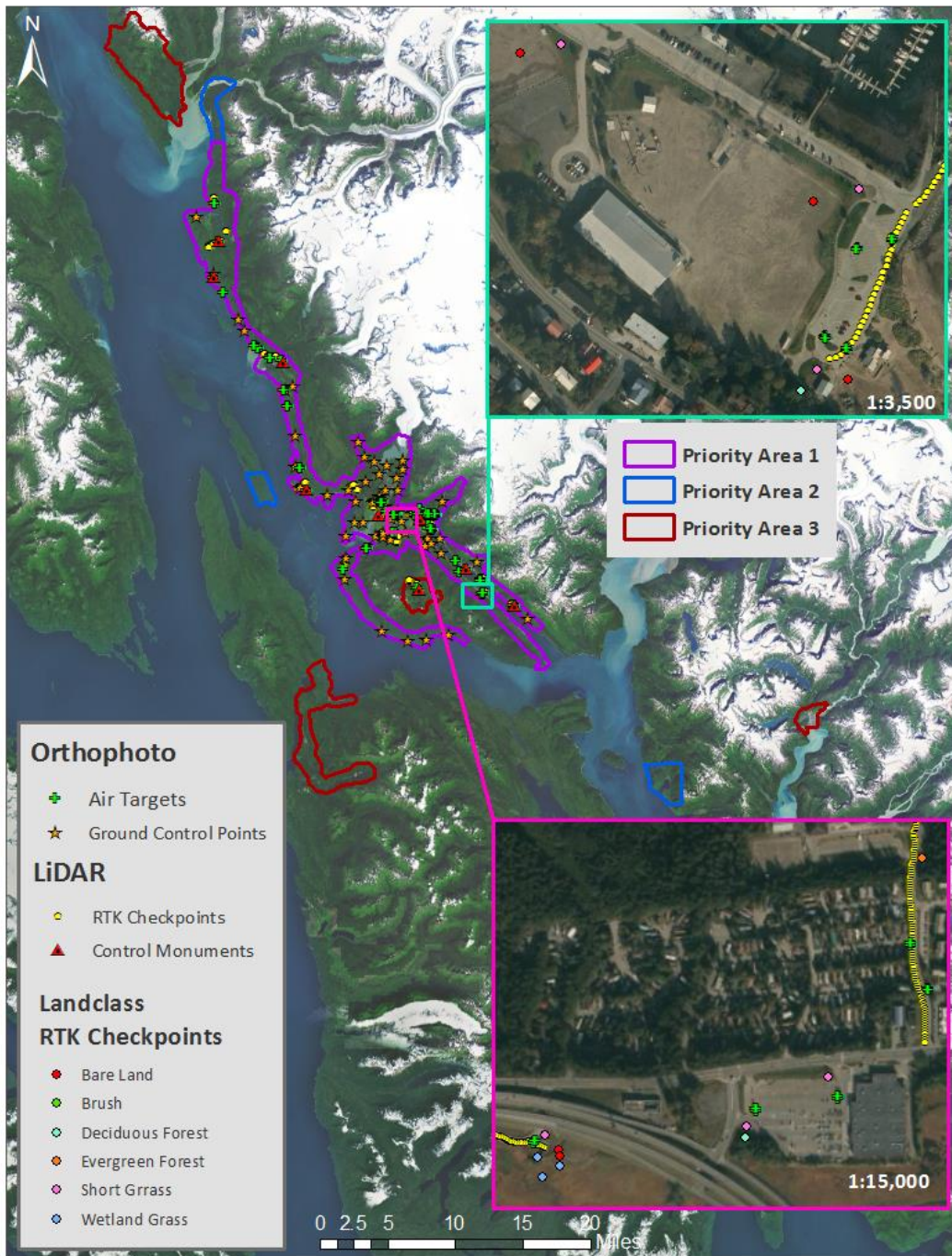


Figure 2: Basestation and RTK checkpoint location map

Land Cover

In addition to control point RTK, land cover check points were taken throughout the study area. Land cover types and descriptions can be referenced in Table 5 and Figure 2. Individual accuracies were calculated for each land-cover type to assess confidence in the LiDAR derived ground models across land cover classes.

Table 5: Land cover descriptions of check points taken for the Juneau Project Area

Land cover type (Database Code)	Example	Description
Bare Ground (BARE)		Perennially barren areas of bedrock, desert pavement, scarps, talus, slides, volcanic material, glacial debris, beaches, and other accumulations of earthen material.
Short Grass (SH_GRASS)		Grass height is below knee.
Wetland Grass (WETLAND_GRASS)		Areas where perennial herbaceous vegetation accounts for 75-100 percent of the cover and the soil or substrate is periodically saturated with or covered with water.

Land cover type (Database Code)	Example	Description
Shrub/Brush (BRUSH)		<p>Vegetation is less than 6 meters tall; Areas dominated by shrubs; shrub canopy accounts for 25-100 percent of the cover. Shrub cover is generally greater than 25 percent when tree cover is less than 25 percent. Shrub cover may be less than 25 percent in cases when the cover of other life forms (e.g. herbaceous or tree) is less than 25 percent and shrubs cover exceeds the cover of the other life forms.</p>
Deciduous Forest (DEC_FOR)		<p>Areas dominated by trees where 75 percent or more of the tree species shed foliage simultaneously in response to seasonal change.</p>
Evergreen Forest (EVER_FOR)		<p>Areas dominated by trees where 75 percent or more of the tree species maintain their leaves all year. Canopy is never without green foliage.</p>

Airborne Survey

LiDAR

The LiDAR survey was accomplished with a Leica ALS60 system mounted in a Cessna Caravan. Table 6 summarizes the settings used to yield an average pulse density of $\geq 4-8$ pulses/m² depending on the area of interest. It is not uncommon for some types of surfaces (e.g. dense vegetation or water) to return fewer pulses to the LiDAR sensor than the laser originally emitted. These discrepancies between native and delivered density will vary depending on terrain, land cover, and the prevalence of water bodies.

As mentioned, limited road access required extended baseline lengths to cover outlying areas of interest.

Table 6: LiDAR specifications and survey settings

LiDAR Survey Settings & Specifications	
Sensor	Leica ALS60
Survey Altitude (AGL)	900-1200 m
Target Pulse Rate	80-106 kHz
Sensor Configuration	Single Pulse in Air (SPiA)
Laser Pulse Diameter	21-28 cm
Mirror Scan Rate	50.3-64 Hz
Field of View	28°
GPS Baselines	P1: ≤ 13 nm P2: ≤ 16 nm P3: ≤ 21 nm
GPS PDOP	≤ 3.0
GPS Satellite Constellation	≥ 6
Maximum Returns	4
Intensity	8-bit
Resolution/Density	P1: 8 pulses/m ² P2 and P3: 4 pulses/m ²
Accuracy	RMSE _z ≤ 15 cm

Leica ALS60 LiDAR sensor



To reduce laser shadowing and increase surface laser painting, all areas were surveyed with an opposing flight line side-lap of $\geq 50\%$ ($\geq 100\%$ overlap). The Leica laser systems record up to four range measurements (returns) per pulse. All discernible laser returns were processed for the output dataset.

To accurately solve for laser point position (geographic coordinates x, y, z), the positional coordinates of the airborne sensor and the attitude of the aircraft were recorded continuously throughout the LiDAR data collection mission. Position of the aircraft was measured twice per second (2 Hz) by an onboard differential GPS unit. Aircraft attitude was measured 200 times per second (200 Hz) as pitch, roll, and yaw (heading) from an onboard inertial measurement unit (IMU). To allow for post-processing correction and calibration, aircraft/sensor position and attitude data are indexed by GPS time.

Digital Imagery

The aerial imagery was collected using an UltraCam Eagle 260 megapixel digital camera mounted in a Cessna 208B Caravan. The UltraCam Eagle is a large format digital aerial camera manufactured by Microsoft Corporation. The system is gyro-stabilized and simultaneously collects panchromatic and multispectral (RGB, NIR) imagery. Panchromatic lenses collect high resolution imagery by illuminating 9 charge coupled device (CCD) arrays, writing 9 raw image files. RGB and NIR lenses collect lower resolution imagery, written as 4 individual raw image files. Level 2 images are created by stitching together raw image data from the 9 panchromatic CCDs and are ultimately combined with the multispectral image data to yield Level 3 pan-sharpened TIFFs.



For the Juneau site, images were collected in 4 spectral bands (red, green, blue, and near infrared) with 60% along track overlap and 30% sidelap between frames. The acquisition flight parameters were designed to yield a native pixel resolution of ≤ 15 -30 cm. The resulting spatial accuracies (RMSE) were routinely ≤ 45 cm at 95% confidence level. Orthophoto specifications are summarized in Table 7.

Table 7: UltraCam Orthophoto specifications

Digital Orthophotography Specifications	
Equipment	UltraCam Eagle
Focal Length	80 mm
Pixel Size	5.2 μ m
Image Size	20,010 x 13,080 pixels
Frame Rate	1.8 seconds
FOV	66° x 46°
Spectral Bands	Red, Green, Blue, NIR
Target Resolution	≤ 15 and 30 cm pixel size
Along Track Overlap	$\geq 60\%$
Planned Height (AGL)	varies
GPS Baselines	P1: ≤ 13 nm P2: ≤ 16 nm P3: ≤ 21 nm
GPS PDOP	≤ 3.0
GPS Satellite Constellation	≥ 6
Horizontal Accuracy	0.06 m
Image	8-bit GeoTiff

LiDAR Data

Upon the LiDAR data's arrival to the office, WSI processing staff initiates a suite of automated and manual techniques to process the data into the requested deliverables. Processing tasks include GPS control computations, smoothed best estimate trajectory (SBET) calculations, kinematic corrections, calculation of laser point position, calibration for optimal relative and absolute accuracy, and a full point classification schema (Table 8 and Figure 3). Processing methodologies are tailored for the landscape and intended application of the point data. A full description of these tasks can be found in Table 9.



Figure 3: Example of a LiDAR cross-section with the full classification schema used for the Juneau Pilot area.



Table 8: ASPRS LAS classification standards applied to the Juneau dataset

Classification Number	Classification Name	Classification Description
2	Ground	Ground that is determined by a number of automated and manual cleaning algorithms to determine the best ground model the data can support
3	Low Vegetation	Any vegetation within 2 feet of the ground surface, includes driftwood in tidal areas
4	Medium Vegetation	Any vegetation between 2 – 6 feet of the ground surface
5	High Vegetation	Any vegetation 6 feet and above the ground surface
6	Buildings	Permanent enclosed structures, includes large water storage tanks
7	Low/Noise	Laser returns that are often associated with birds or artificial points below the ground surface also known as “pits”
9	Water	All water (closed waterbodies, ocean and river)
10	Ignored Ground	Ground points proximate to water’s edge breaklines, ignored for correct model creation
11	Withheld	Laser returns that have intensity values of 0 or 255
12	Mobile	Non-permanent features (Cars, boats, sheds (<15m ²), play structures, livestock, woodpiles, etc.)
13	Utilities	Features not considered as Buildings or Mobile (Powerlines, docks, fences)
14	Bridges	Structures spanning and providing passage over a river, chasm, road, etc.
15	Ice	Mendenhall glacier and associate icebergs in Mendenhall Lake
16	Snow (based on photos) ²	Ground classified points identified by as being areas where snow was likely present during the LiDAR acquisition.
17	Decks	Open, unroofed porch or platform extending from a house or other building, includes balconies which are railed elevated platforms projecting from the wall of a building
18	Awnings	Canvas or other material stretched on a frame and used to keep the sun or rain off a storefront, window, doorway, or deck

² Classification of snow based on the LiDAR was not possible due to the lack of a distinct intensity value from the melting snow. Due to the later acquisition time frame of the photos, snow classing should only be used as a general indication of where snow was present on the ground during the LiDAR acquisition. These points were used as ground for all model creation.

Table 9: LiDAR processing workflow

LiDAR Processing Step	Software Used
Resolve kinematic corrections for aircraft position data using kinematic aircraft GPS and static ground GPS data.	Waypoint GPS v.8.3 Trimble Business Center v.3.00 Geographic Calculator 2013
Develop a smoothed best estimate of trajectory (SBET) file that blends post-processed aircraft position with attitude data. Sensor head position and attitude are calculated throughout the survey. The SBET data are used extensively for laser point processing.	IPAS TC v.3.1
Calculate laser point position by associating SBET position to each laser point return time, scan angle, intensity, etc. Create raw laser point cloud data for the entire survey in *.las (ASPRS v. 1.2) format. Data are converted to orthometric elevations (NAVD88) by applying a Geoid12 correction.	ALS Post Processing Software v.2.74
Import raw laser points into manageable blocks (less than 500 MB) to perform manual relative accuracy calibration and filter erroneous points. Ground points are then classified for individual flight lines (to be used for relative accuracy testing and calibration).	TerraScan v.13.008
Using ground classified points per each flight line, the relative accuracy is tested. Automated line-to-line calibrations are then performed for system attitude parameters (pitch, roll, heading), mirror flex (scale) and GPS/IMU drift. Calibrations are calculated on ground classified points from paired flight lines and results are applied to all points in a flight line. Every flight line is used for relative accuracy calibration.	TerraMatch v.13.002
Classify resulting data to ground and other client designated ASPRS classifications (Table 8). Assess statistical absolute accuracy via direct comparisons of ground classified points to ground RTK survey data.	TerraScan v.13.008 TerraModeler v.13.002
Generate bare earth models as triangulated surfaces. Highest hit models were created as a surface expression of all classified points (excluding the noise and withheld classes). All surface models were exported as GeoTIFFs at a 1-meter/3-foot pixel resolution.	TerraScan v.13.008 ArcMap v. 10.1 TerraModeler v.13.002
Correct intensity values for variability and export intensity images as GeoTIFFs at a 0.5 meter/1.5-foot pixel resolution.	TerraScan v.13.008 ArcMap v. 10.1 TerraModeler v.13.002

Intensity Normalization

Laser return intensity is a unitless value corresponding to the reflectivity and composition of the target. Derived from the laser return voltage, it is initially stored as an integer value from 0 to 255 (8-bit). Differences in the magnitude of intensity values across similar targets is a function of receiver auto gain control (AGC), atmospheric (transmissivity and target range), laser power, and the angle of incidence. These components influence intensity at different rates and magnitudes, with AGC comprising the majority of influence. The result is variability in returned intensity values across the landscape that can reduce the utility of these data for analysis.

Variability as a result of each of these components is reduced mathematically to arrive at a normalized intensity value that approaches a true radiometric value for each discrete LiDAR return. WSI employs proprietary software to normalize intensity values for AGC and atmospheric effects. The contribution of each pulse's angle of incidence with the ground surface is also normalized to a limited extent using scanner angle as a proxy. Corrections for the angle of incidence and laser power are still being actively researched, so some intensity variability may be observed in the dataset, particularly on very steep slopes. A representative sample of the intensity normalization achieved for this project is shown below (Figure 4).

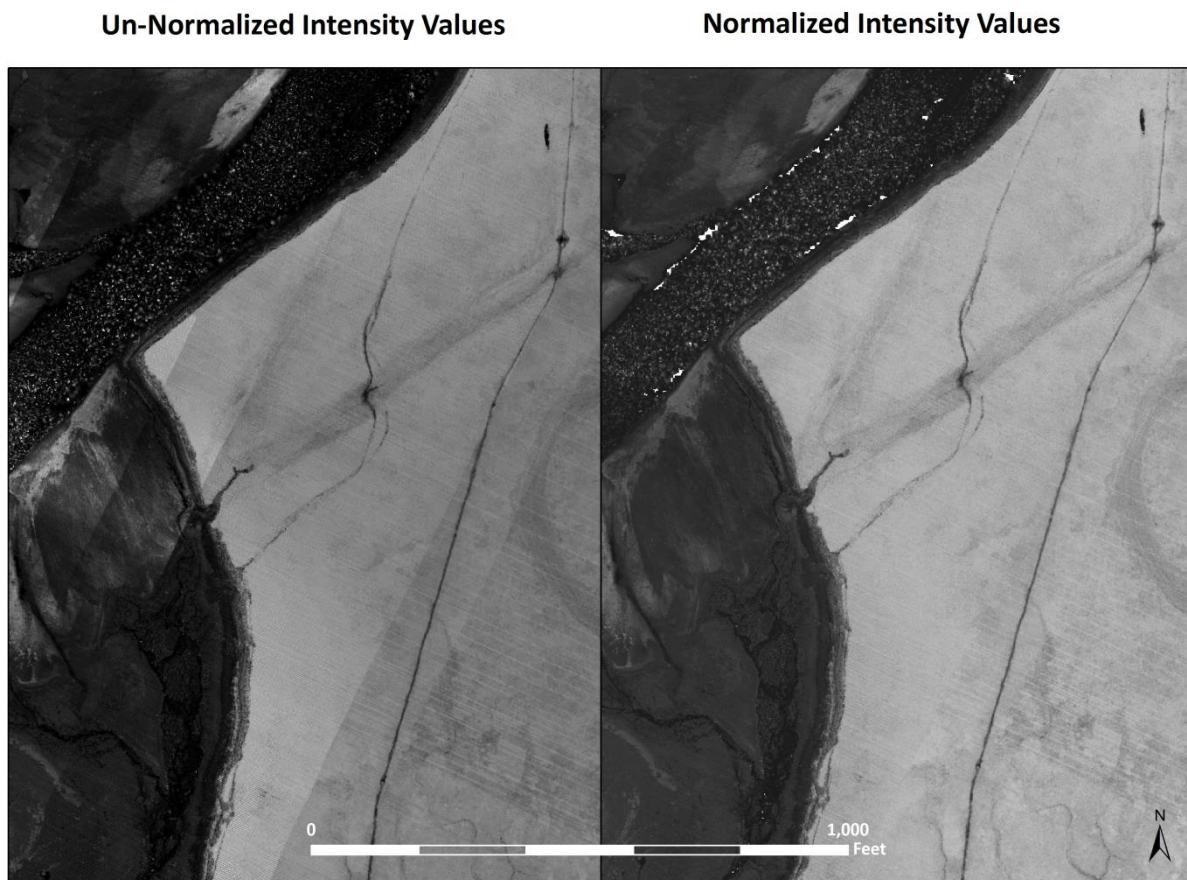


Figure 4: Comparison of normalized and un-normalized intensities

Feature Extraction

Contours

Contour generation from LiDAR point data requires a thinning operation in order to reduce contour sinuosity. The thinning operation reduces point density where topographic change is minimal (flat surfaces) while preserving resolution where topographic change is present. These model key points are selected from the ground model every 20 feet with the spacing decreased in regions with high surface curvature (Z tolerance of 0.15 feet). Generation of model key points eliminates redundant detail in terrain representation, particularly in areas of low relief, and provides for a more manageable dataset. Contours are then produced through TerraModeler by interpolating between the model key points at even elevation increments.

Elevation contour lines are then intersected with ground point density rasters and a confidence field is added to each contour line. Contours crossing areas of high point density have high confidence levels. Contours crossing areas with low ground point densities preclude the generation of contours at the specified interval resulting in contours being classified as 'low' confidence. These areas with low ground point density are commonly beneath buildings and bridges, in locations with dense vegetation, over water, and in other areas where laser penetration to the ground surface is impeded (Figure 5).

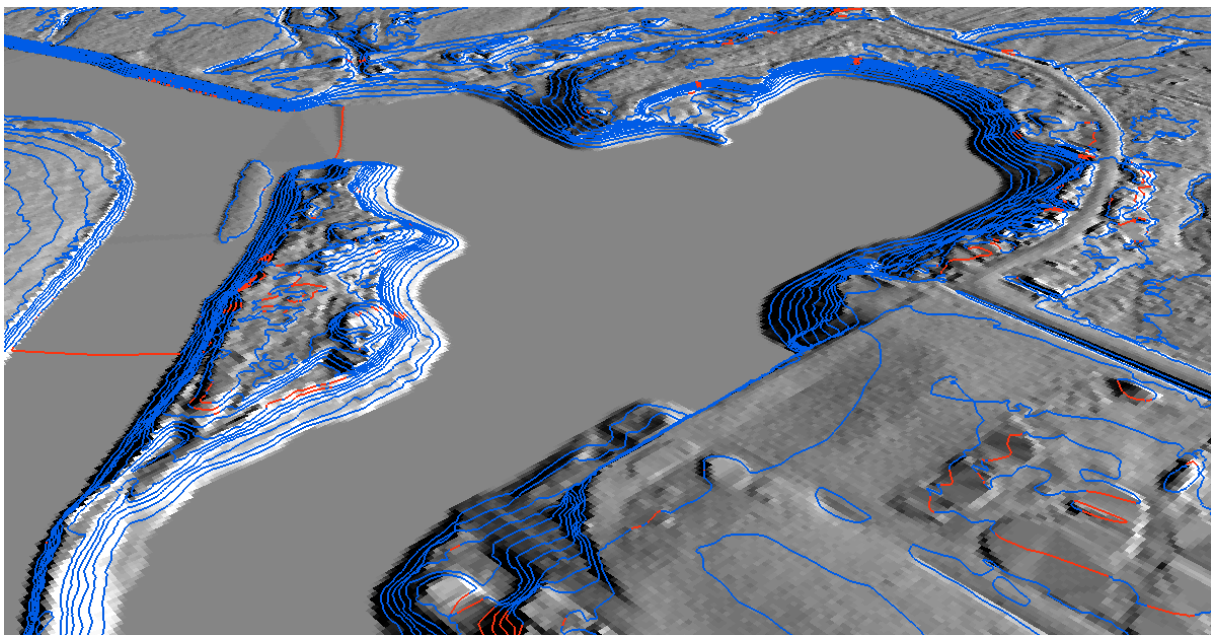


Figure 5: Contours draped over the Juneau bare earth elevation model. Blue contours represent high confidence while the red contours represent low confidence.

Hydro-flattening

WSI created hydro-flattening breaklines for water surfaces greater than ~100 feet in width. The water's edge was detected using an algorithm which weights LiDAR-derived slopes, intensities, and return densities to detect the water's edge. Elevations were assigned to the water's edge through neighborhood statistics identifying the lowest LiDAR return from the water surface. Lakes were assigned a consistent elevation for an entire polygon while rivers were assigned consistent elevations on opposing banks and smoothed to ensure downstream flow through the entire river channel. These breaklines were incorporated into the hydro-flattened DEM by enforcing triangle edges (adjacent to the breakline) to the elevation values derived from the breakline. This implementation corrected interpolation along the hard edge. Water surfaces were obtained from a TIN of the 3-D water edge breaklines resulting in the final hydroflattened model (Figure 6).

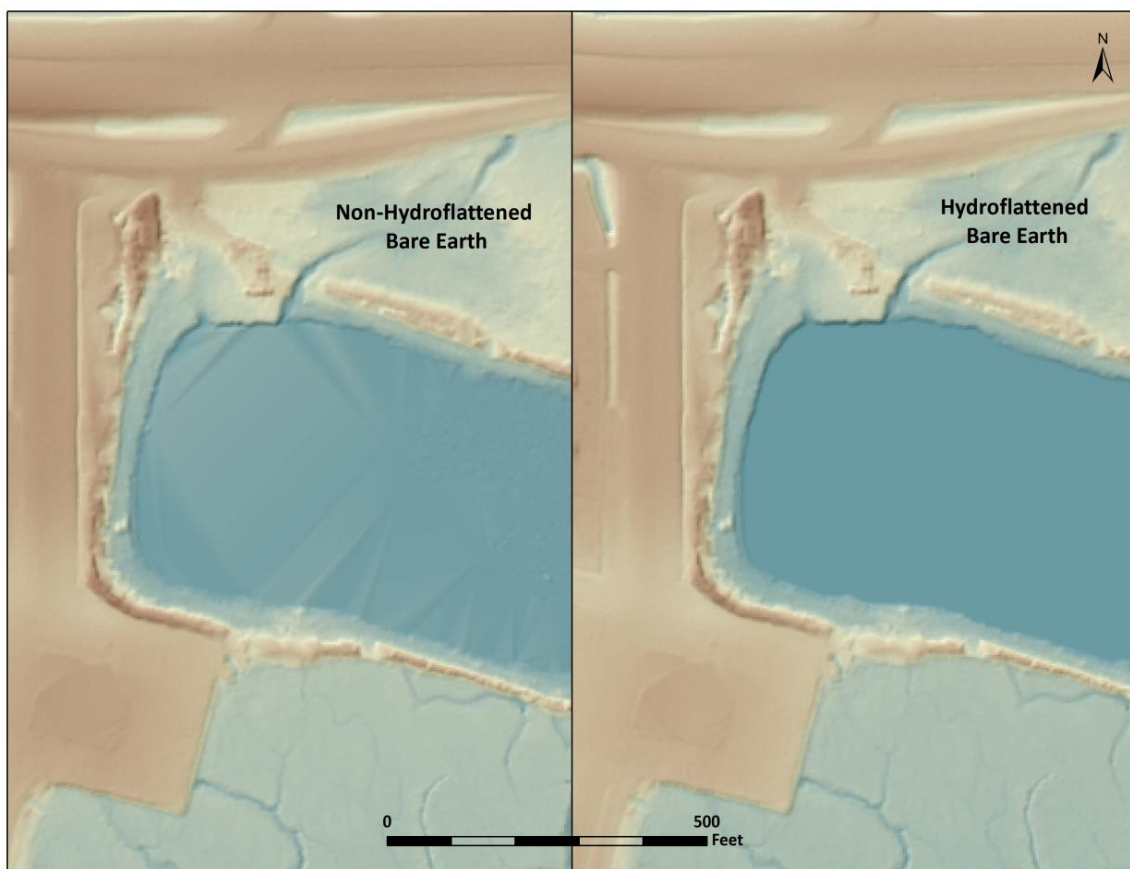


Figure 6: Example of hydro-flattening in the Juneau LiDAR dataset

Digital Imagery

As with the NIR LiDAR, the collected digital photographs went through multiple processing steps to create final orthophoto products. Initially, image radiometric values were calibrated to specific gain and exposure settings. Photo position and orientation were then calculated by linking the time of image capture to the smoothed best estimate of trajectory (SBET) file created during LiDAR post-processing. Within Leica Photogrammetry Suite (LPS), an automated aerial triangulation was performed to tie images together and adjust the photo block to align with ground control.

Adjusted images were orthorectified using the LiDAR-derived ground model to remove displacement effects from topographic relief inherent in the imagery and individual orthorectified TIFFs were blended together to remove seams. The final mosaics were corrected for any remaining radiometric differences between images using Inpho’s OrthoVista. The processing workflow for orthophotos is summarized in Table 10.

Table 10: Orthophoto processing workflow

Orthophoto Processing Step	Software Used
Resolve GPS kinematic corrections for the aircraft position data using kinematic aircraft GPS (collected at 2HS) and static ground GPS (1Hz) data collected over geodetic controls.	POSPac MMS v. 6.1
Develop a smooth best estimate trajectory (SBET) file that blends post-processed aircraft position with attitude data. Sensor heading, position, and attitude are calculated throughout the survey.	POSPac MMS v. 5.4
Create an exterior orientation file (EO) for each photo image with omega, phi, and kappa.	POSPac MMS v. 6.1
Convert Level 00 raw imagery data into geometrically corrected Level 02 image files.	UltraMap 2.3.2
Apply radiometric adjustments to Level 02 image files to create Level 03 Pan-sharpened TIFFs.	UltraMap 2.3.2
Apply EO to photos, measure ground control points and perform aerial triangulation.	LPS 2013
Import DEM, orthorectify and clip triangulated photos to the specified area of interest.	LPS 2013
Mosaic orthorectified imagery, blending seams between individual photos and correcting for radiometric differences between photos.	Inpho v. 5.5

LiDAR Density

The sensor was set to acquire a native density of 8 points/m² in Priority Area 1 and 4 points/m² in Priority Areas 2 and 3. Depending on the nature of the terrain, the first returned echo will be the highest hit surface. In vegetated areas, the first return surface will represent the top of the canopy, while in clearings or on paved roads, the first return surface will represent the ground. The ground density differs from the first return density due to the fact that in vegetated areas, fewer returns may penetrate the canopy. The ground classification is generally determined by first echo returns in non-vegetated areas combined with last echo returns in vegetated areas.

The pulse density distribution will vary within the study area due to laser scan pattern and flight conditions. Additionally, some types of surfaces (i.e. breaks in terrain, water, steep slopes) may return fewer pulses to the sensor than originally emitted by the laser.

The average first-return density for the LiDAR data for Priority Area 1 was 1.13 points/ft² (12.18 points/m²) with ground densities of 0.13 points/ft² (1.43 points/m²) (Table 11). In Priority Areas 2 and 3, the average first return density was 0.67 points/ft² (7.17 points/m²) with ground densities of 0.12 points/ft² (1.24 points/m²). The statistical distribution of first returns (Figure 7 and Figure 8) and classified ground points (Figure 9 and Figure 10) are portrayed below. Also presented are the spatial distribution of average first return densities (Figure 11) and ground point densities (Figure 12) for each 100mx100m cell.

Table 11: Average LiDAR point densities

Classification	P1 Point Density (8 pt. spec.)	P2 & P3 Point Density (4 pt. spec.)
First-Return	1.13 points/ft ² 12.18 points/m ²	0.67 points/ft ² 7.17 points/m ²
Ground Classified	0.13 points/ft ² 1.43 points/m ²	0.12 points/ft ² 1.24 points/m ²

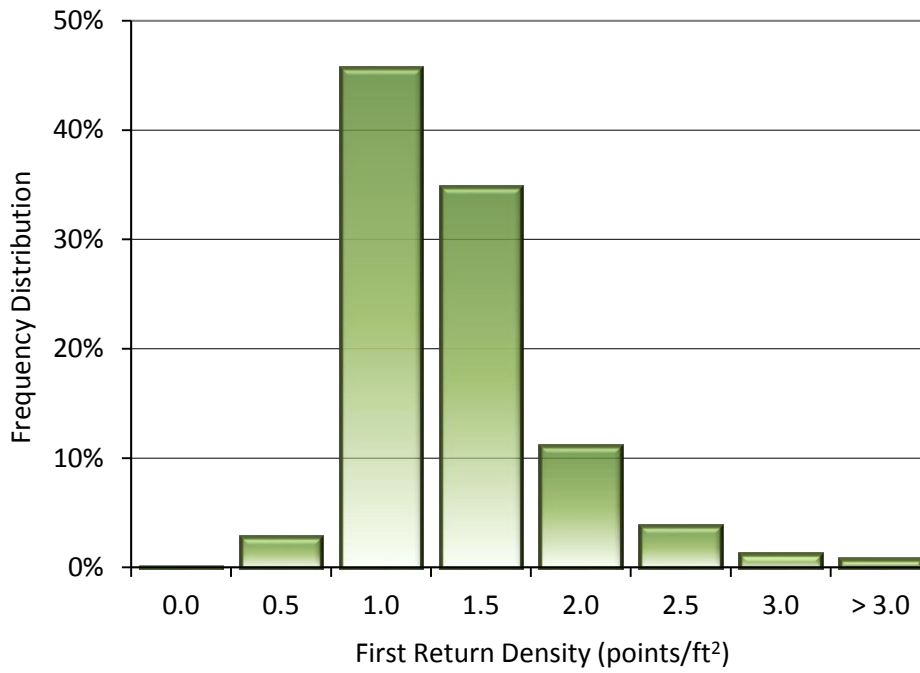


Figure 7: Frequency distribution of first return densities (native densities) of Priority Area 1

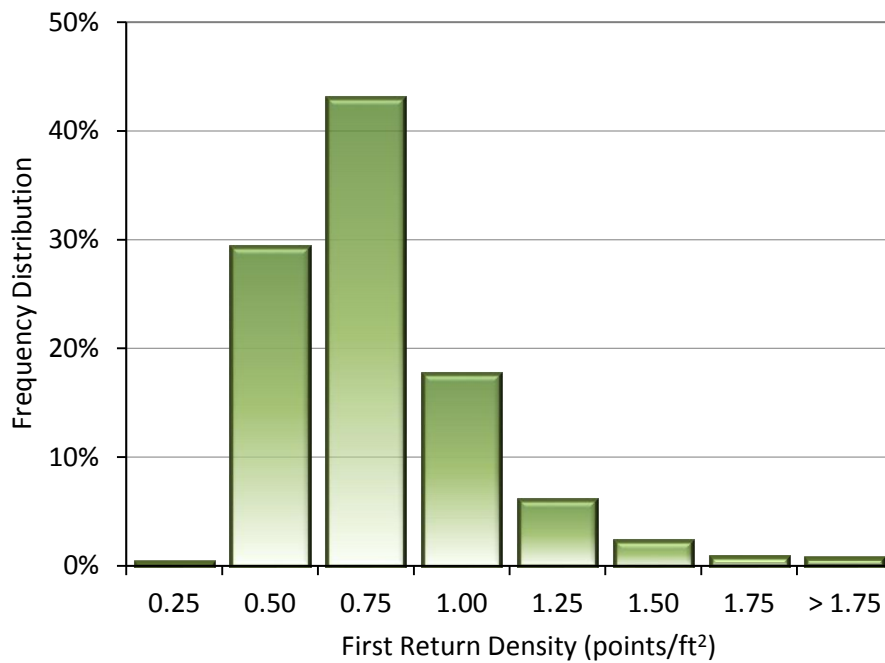


Figure 8: Frequency distribution of first return densities (native densities) of Priority Areas 2 and 3

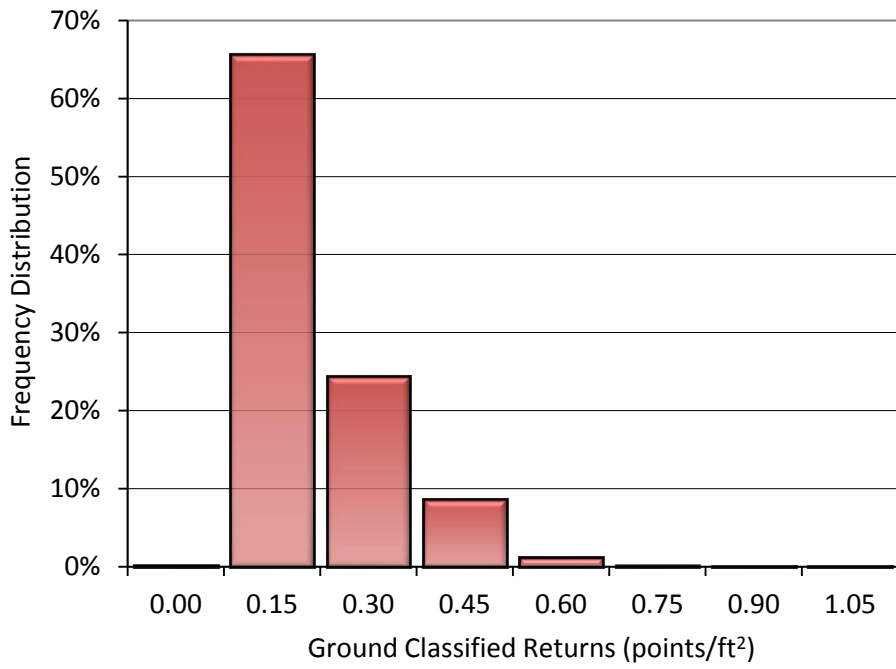


Figure 9: Frequency distribution of ground return densities of Priority Area 1

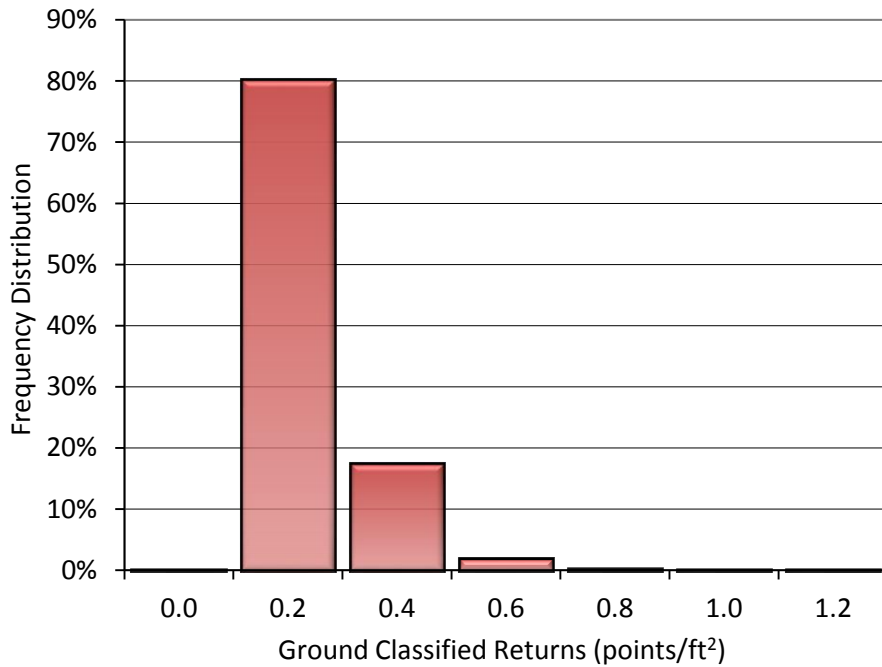


Figure 10: Frequency distribution of ground return densities of Priority Areas 2 and 3

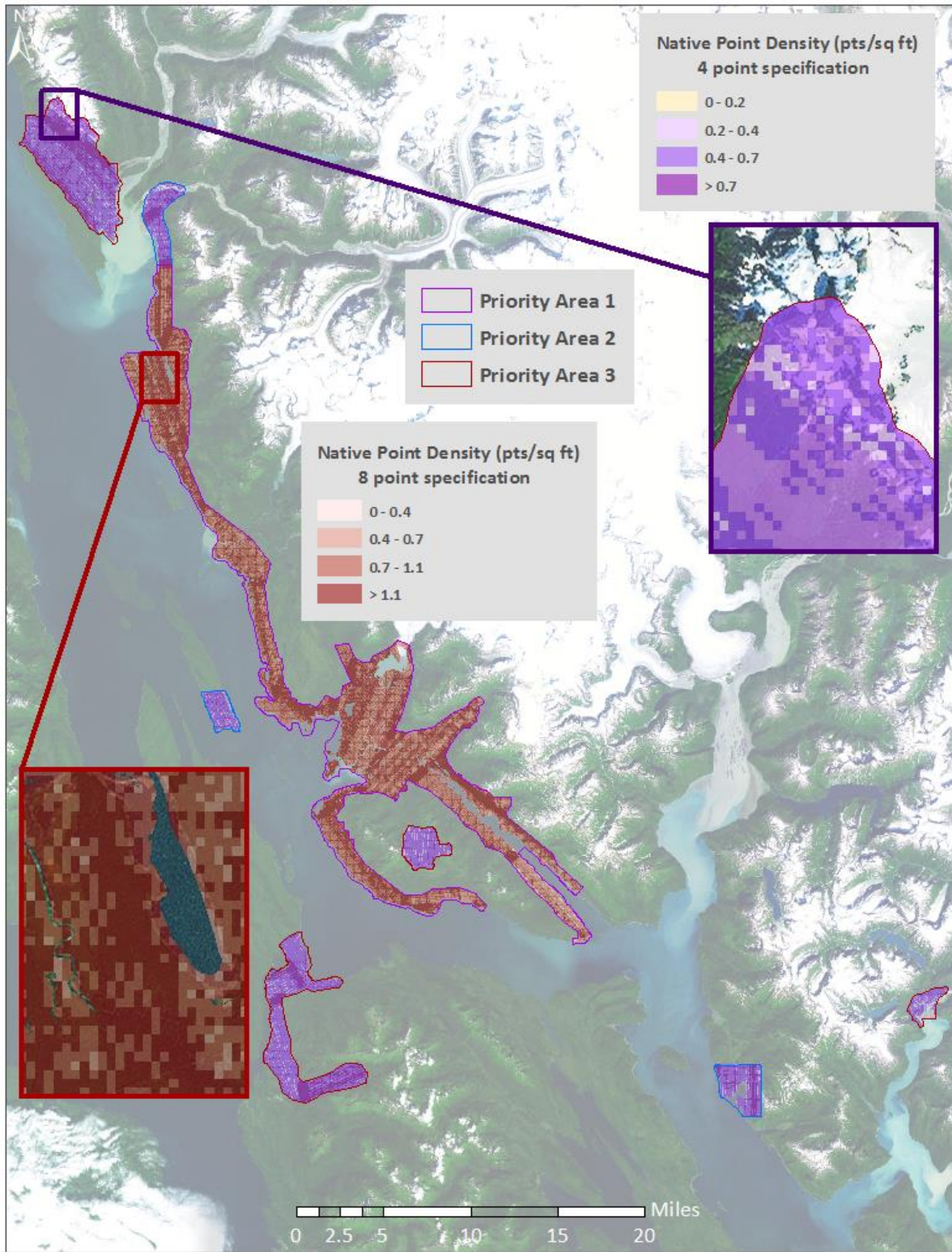


Figure 11: Native density map for the Juneau area (100mx100m cells)

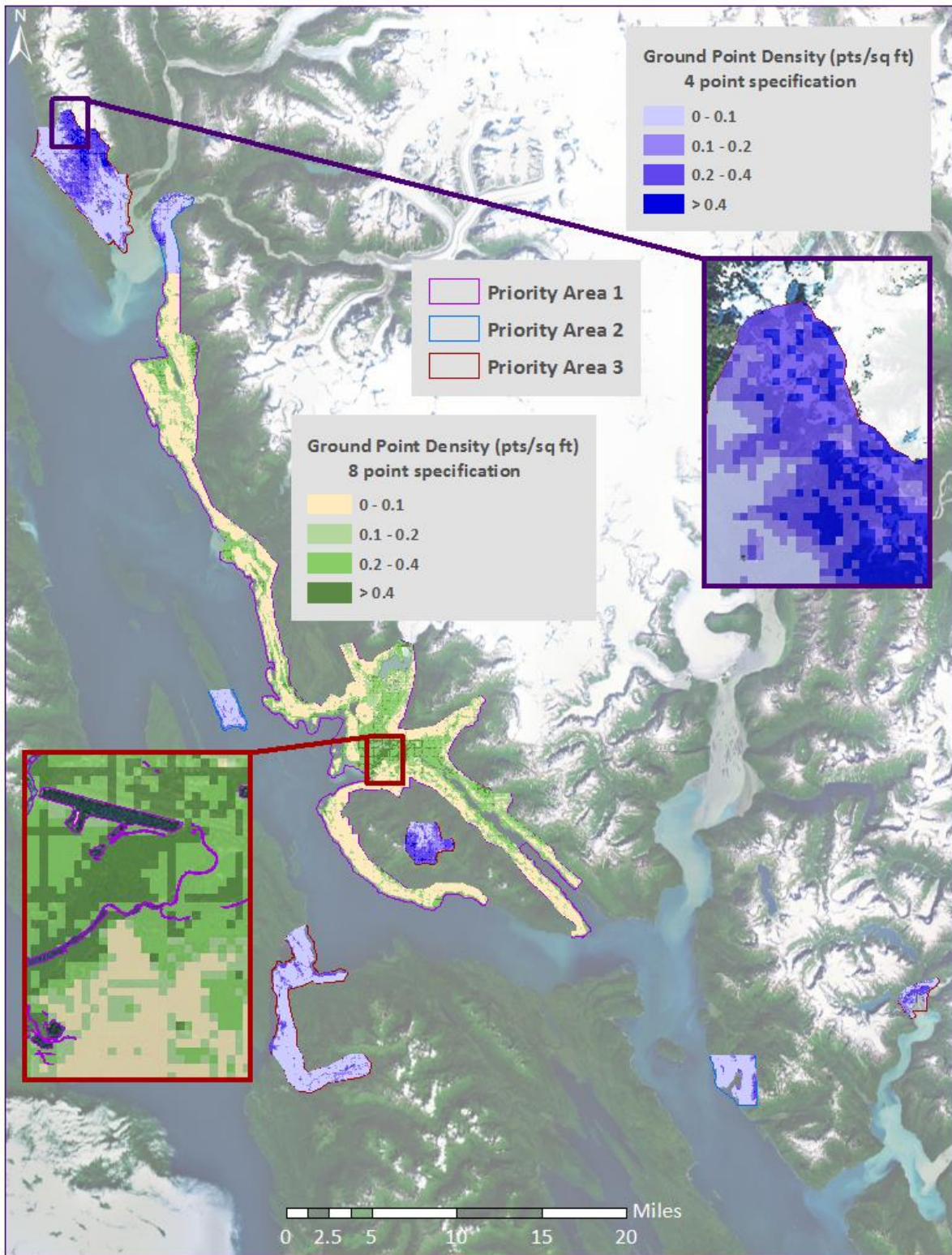


Figure 12: Ground density map for the Juneau area (100mx100m cells)

LiDAR Accuracy Assessments

The accuracy of the LiDAR data collection can be described in terms of absolute accuracy (the consistency of the data with external data sources) and relative accuracy (the consistency of the dataset with itself). See Appendix C for further information on sources of error and operational measures used to improve relative accuracy.

LiDAR Absolute Accuracy

Vertical absolute accuracy was primarily assessed from RTK ground check point (GCP) data collected on open, bare earth surfaces with level slope (<20°). Fundamental Vertical Accuracy (FVA) reporting is designed to meet guidelines presented in the FGDC National Standard for Spatial Data Accuracy³. FVA compares known RTK ground survey check points to the triangulated ground surface generated by the LiDAR points. FVA is a measure of the accuracy of LiDAR point data in open areas where the LiDAR system has a “very high probability” of measuring the ground surface and is evaluated at the 95% confidence interval (1.96 σ).

Absolute accuracy is described as the mean and standard deviation (sigma σ) of divergence of the ground surface model from ground survey point coordinates. These statistics assume the error for x, y, and z is normally distributed, and therefore the skew and kurtosis of distributions are also considered when evaluating error statistics. For the cumulative Juneau project area, 3,095 RTK points were collected in total resulting in an average accuracy of -0.014 feet (-0.004 meters) (Table 12, Figure 13).

Table 12: Absolute and relative accuracies assessed across the project area

Absolute Accuracy		
	feet	meters
Sample	3,095 points	3,095 points
Average	-0.014	-0.004
Median	-0.013	-0.004
RMSE	0.098	0.030
Standard Deviation (1σ)	0.098	0.030
FVA (95%) (1.96*RMSE)	0.192	0.059

³ Federal Geographic Data Committee, Geospatial Positioning Accuracy Standards (FGDC-STD-007.3-1998). Part 3: National Standard for Spatial Data Accuracy. <http://www.fgdc.gov/standards/projects/FGDC-standards-projects/accuracy/part3/chapter3>

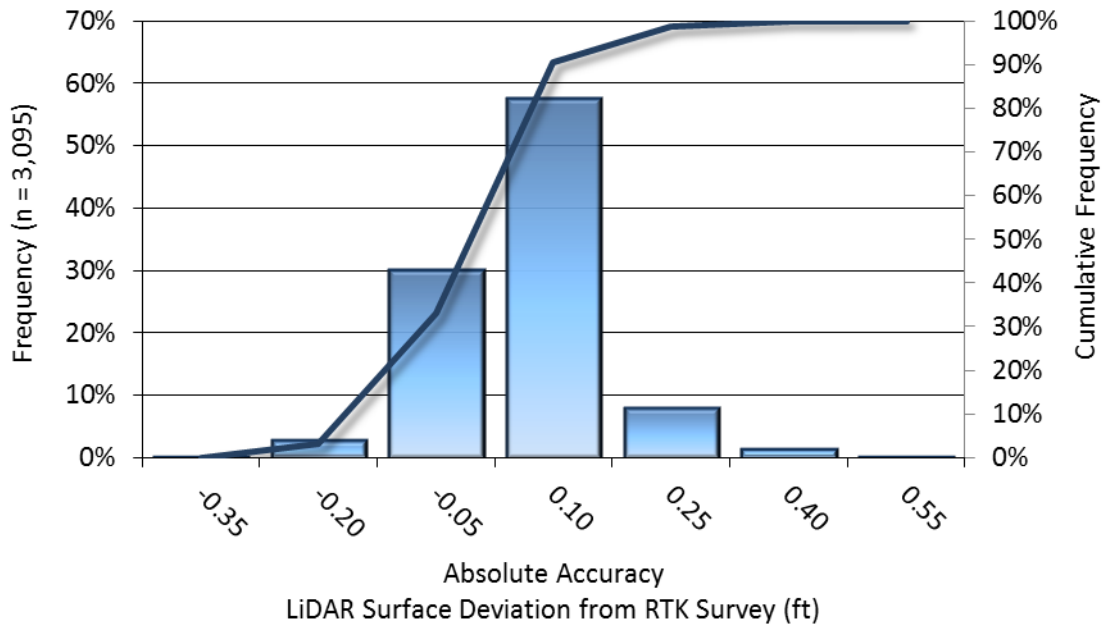


Figure 13: Frequency histogram for LiDAR surface deviation from RTK values

In addition to hard surface RTK, 167 land cover check points were taken throughout the survey site. Land cover types and descriptions can be referenced in Table 5. Individual accuracies were calculated for each land-cover type to assess confidence in the LiDAR derived ground models across land-cover classes (Table 13).

Table 13: Land cover SVA for the Juneau project. All values in feet.

Vertical Accuracy of Land Cover Classes						
Land Cover	Sample Size (n)	Mean Dz (feet)	RMSE	Standard Deviation (1σ)	1.96 σ	95 th Percentile (SVA)
Bare Earth	35	0.019	0.113	0.113	0.222	0.235
Brush	23	0.138	0.403	0.387	0.758	0.775
Deciduous Forest	21	0.091	0.221	0.207	0.405	0.400
Evergreen Forest	29	0.062	0.197	0.190	0.373	0.417
Short Grass	37	0.070	0.175	0.163	0.319	0.429
Wetland Grass	22	0.172	0.203	0.111	0.218	0.348

Consolidated Vertical Accuracy (CVA) for this dataset was 0.064 meters (0.210 feet) at the 95th percentile. CVA was calculated using all hard surface RTK check points and all land cover class points (Bare Earth, Brush, Deciduous Forest, Evergreen Forest, Short Grass, and Wetland Grass) (Table 14).

Table 14: Consolidated Vertical Accuracy (CVA) of all hard surface RTK and land cover class check points

Consolidated Vertical Accuracy		
	feet	meters
Sample	3,262	3,262
Average	-0.009	-0.003
Median	-0.010	-0.003
RMSE	0.108	0.033
Standard Deviation (1σ)	0.108	0.033
95 th Percentile	0.210	0.064

LiDAR Relative Accuracy

Relative accuracy refers to the internal consistency of the data set as a whole: the ability to place an object in the same location given multiple flight lines, GPS conditions, and aircraft attitudes. When the LiDAR system is well calibrated, the swath-to-swath divergence is low (<0.10 meters). The relative accuracy is computed by comparing the ground surface model of each individual flight line with its neighbors in overlapping regions. The average line to line relative accuracy for the Juneau Study Area was 0.14 feet (Table 15, Figure 14).

Table 15: Relative Accuracy

Relative Accuracy		
	feet	meters
Sample	607 surfaces	607 surfaces
Average	0.043	0.140
Median	0.043	0.141
RMSE	0.053	0.175
Standard Deviation (1σ)	0.022	0.071
1.96σ	0.042	0.138

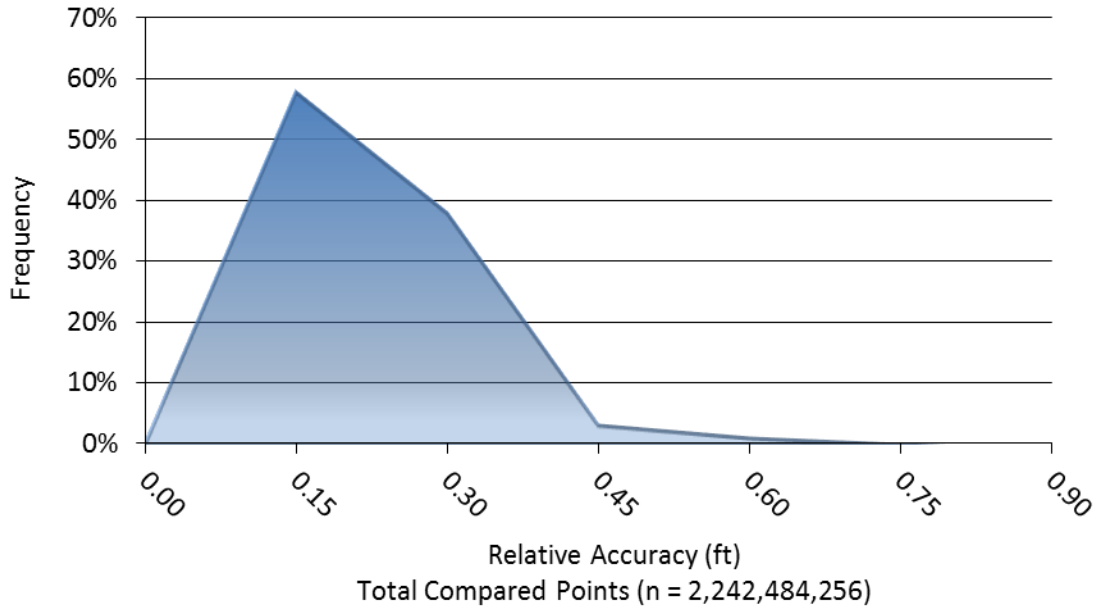
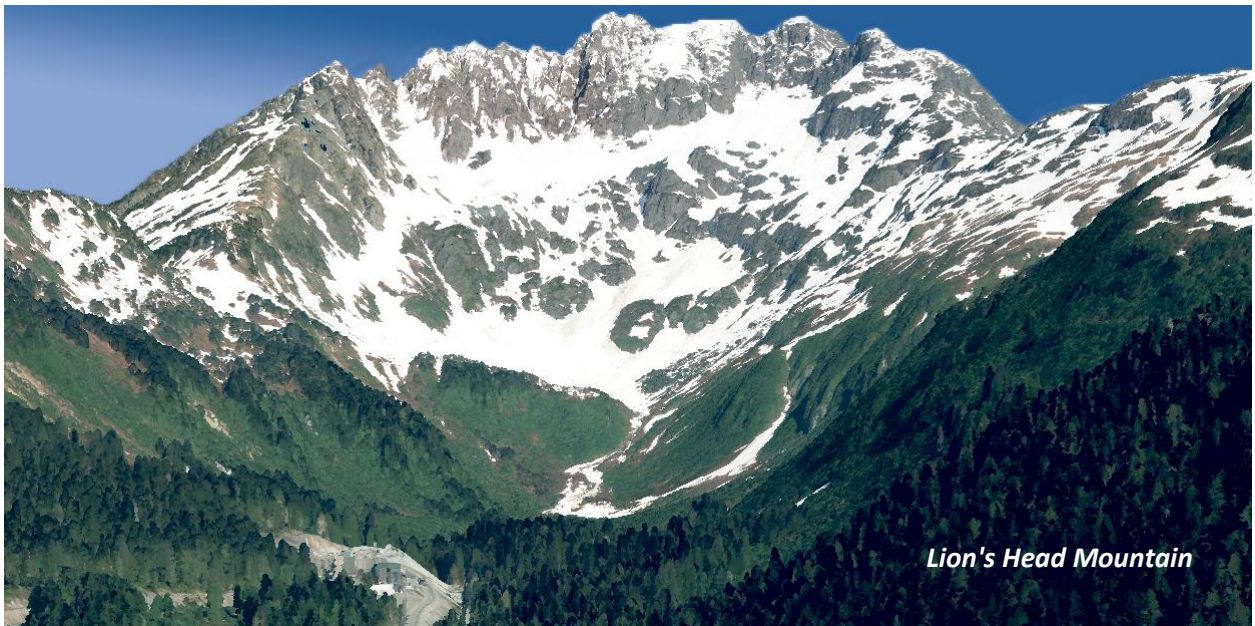


Figure 14: Frequency plot for relative accuracy between flight lines



Digital Imagery Accuracy Assessment

Image accuracy is measured by both air target locations and independent ground check points. Air target GPS points were measured against the placement of the air target in the imagery. In addition, ground check points were identified on the LiDAR intensity images in areas of clear visibility. Once the ground check points were identified in the intensity images the exact spot was identified in the orthophotography, and the displacement was recorded for further statistical analysis.

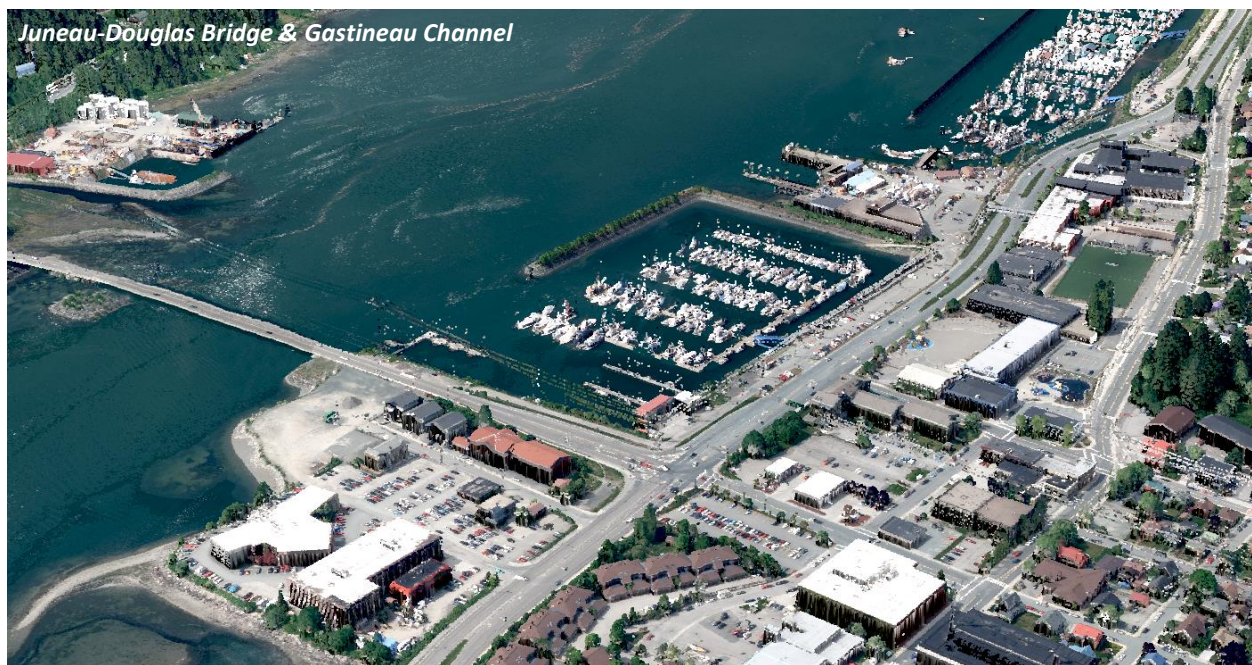
The cumulative orthophoto horizontal accuracy (RMSE) for the Juneau Priority Area 1 was 0.55 feet (0.17 meters) measured by ground control points and 0.30 feet (0.09 meters) measured by air targets, meeting our accuracy standard of <3 pixels (0.45 meters) (Table 16). For Priority Areas 2 and 3, the cumulative horizontal accuracy was 0.94 feet (0.29 meters) measured by ground control points and 0.16 feet (0.05 meters) measured by air targets (Table 17). Figure 15 and Figure 16 contain scatterplots showing congruence between LiDAR intensity images and orthophotos in aerial target locations, while Figure 17 and Figure 18 shows an example of the co-registration of the orthophotos to the LiDAR intensity images.

Table 16: Orthophotography accuracy statistics for the Juneau Priority Area 1

Priority Area 1 Photo Accuracy							
		Check Points _x	Check Points _y	Check Points _{xy}	Air Targets _x	Air Targets _y	Air Targets _{xy}
<i>Sample size</i>		53			23		
Mean	<i>ft</i>	0.104	0.027	0.107	-0.020	0.013	0.024
	<i>m</i>	0.032	0.008	0.033	-0.006	0.004	0.007
Avg. mag.	<i>ft</i>	0.349	0.346	0.491	0.197	0.182	0.268
	<i>m</i>	0.106	0.105	0.150	0.060	0.055	0.082
RMSE	<i>ft</i>	0.388	0.386	0.547	0.224	0.199	0.300
	<i>m</i>	0.118	0.118	0.167	0.068	0.061	0.091
Std Dev (1σ)	<i>ft</i>	0.378	0.389	0.542	0.228	0.203	0.305
	<i>m</i>	0.115	0.119	0.165	0.069	0.062	0.093
1.96σ	<i>ft</i>	0.741	0.762	1.063	0.447	0.398	0.599
	<i>m</i>	0.226	0.232	0.324	0.136	0.121	0.183

Table 17: Orthophotography accuracy statistics for Priority Areas 2 and 3

Priority Areas 2 and 3 Photo Accuracy							
		Check Points _x	Check Points _y	Check Points _{xy}	Air Targets _x	Air Targets _y	Air Targets _{xy}
Sample size		42			2		
mean	ft	-0.066	-0.104	0.123	-0.082	-0.082	0.116
	m	-0.020	-0.032	0.037	-0.025	-0.025	0.035
avg. mag.	ft	0.394	0.463	0.608	0.082	0.082	0.116
	m	0.120	0.141	0.185	0.025	0.025	0.035
RMSE	ft	0.634	0.688	0.936	0.116	0.116	0.164
	m	0.193	0.210	0.285	0.035	0.035	0.050
1σ	ft	0.638	0.689	0.939	0.116	0.116	0.164
	m	0.194	0.210	0.286	0.035	0.035	0.050
1.96σ	ft	1.250	1.350	1.840	0.227	0.227	0.321
	m	0.381	0.411	0.561	0.069	0.069	0.098



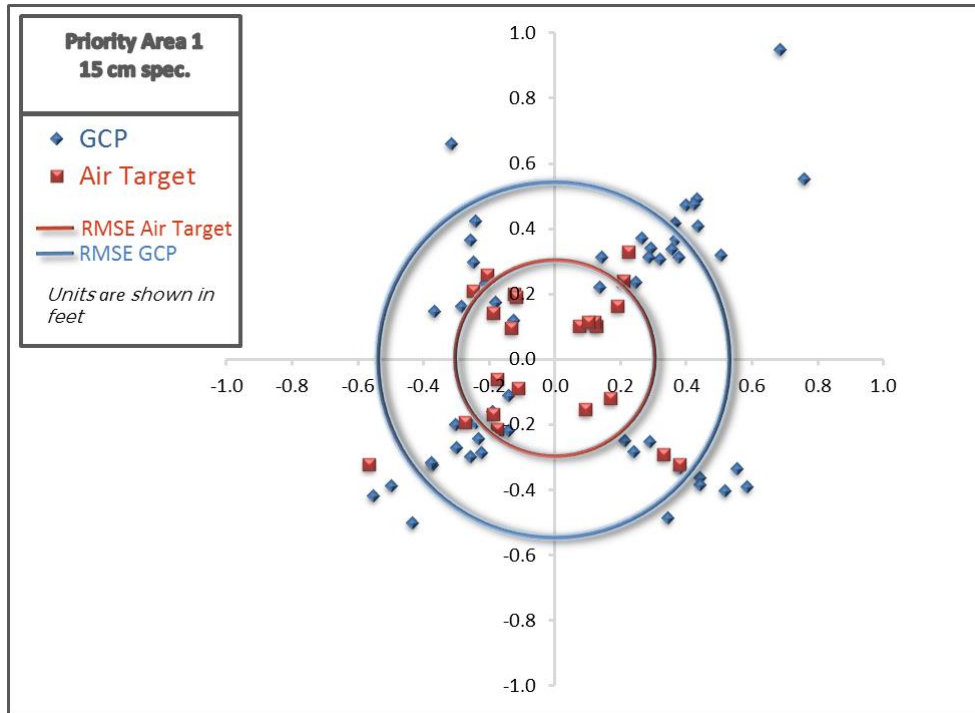


Figure 15: Scatterplot displaying the XY deviation of aerial targets aligned with the orthophoto imagery when compared against the LiDAR intensity images.

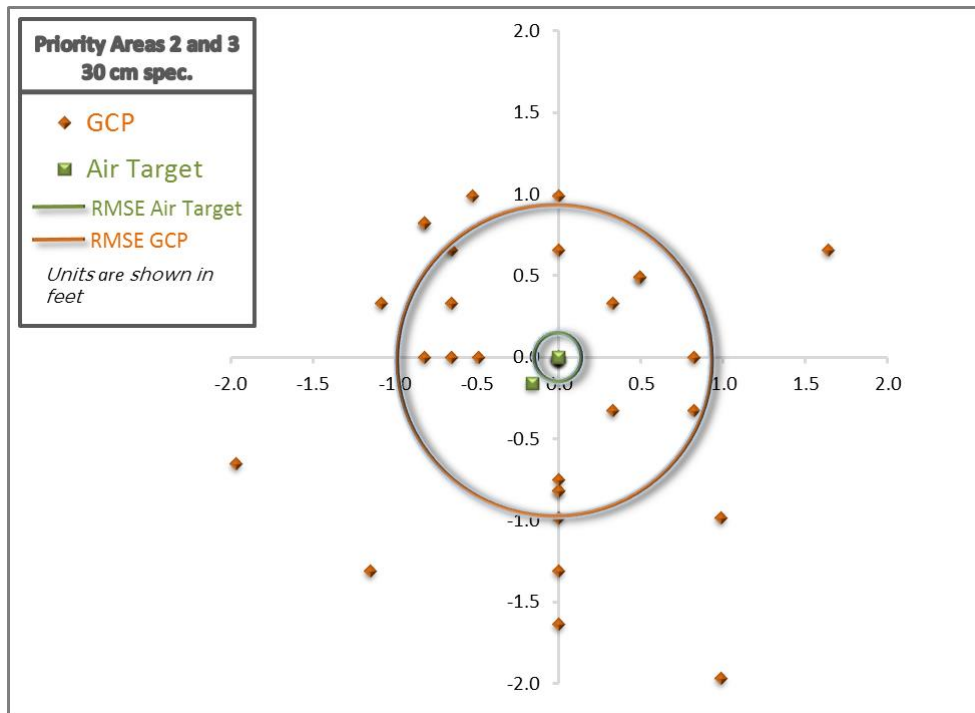


Figure 16: Scatterplot displaying the XY deviation of aerial targets aligned with the orthophoto imagery when compared against the LiDAR intensity images.

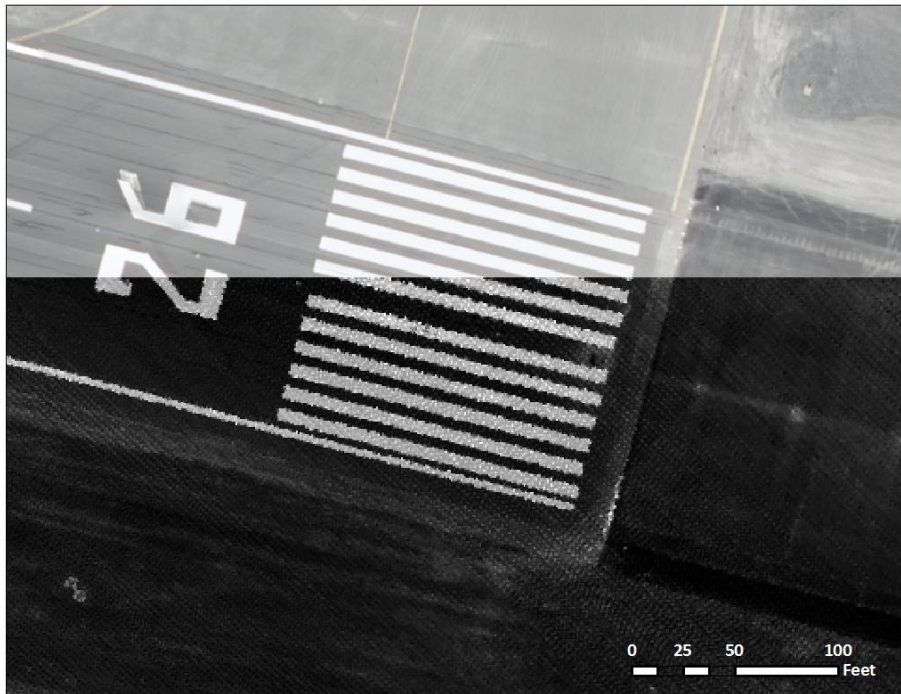


Figure 17: Image displaying the co-registration between the LiDAR intensity image and the 15 cm orthophoto at a location within the Juneau Priority 1 area.



Figure 18: Image displaying the co-registration between the LiDAR intensity image and the 30 cm orthophoto at a location within the Juneau LiDAR and Imagery Priority 1 area.

SELECTED IMAGES

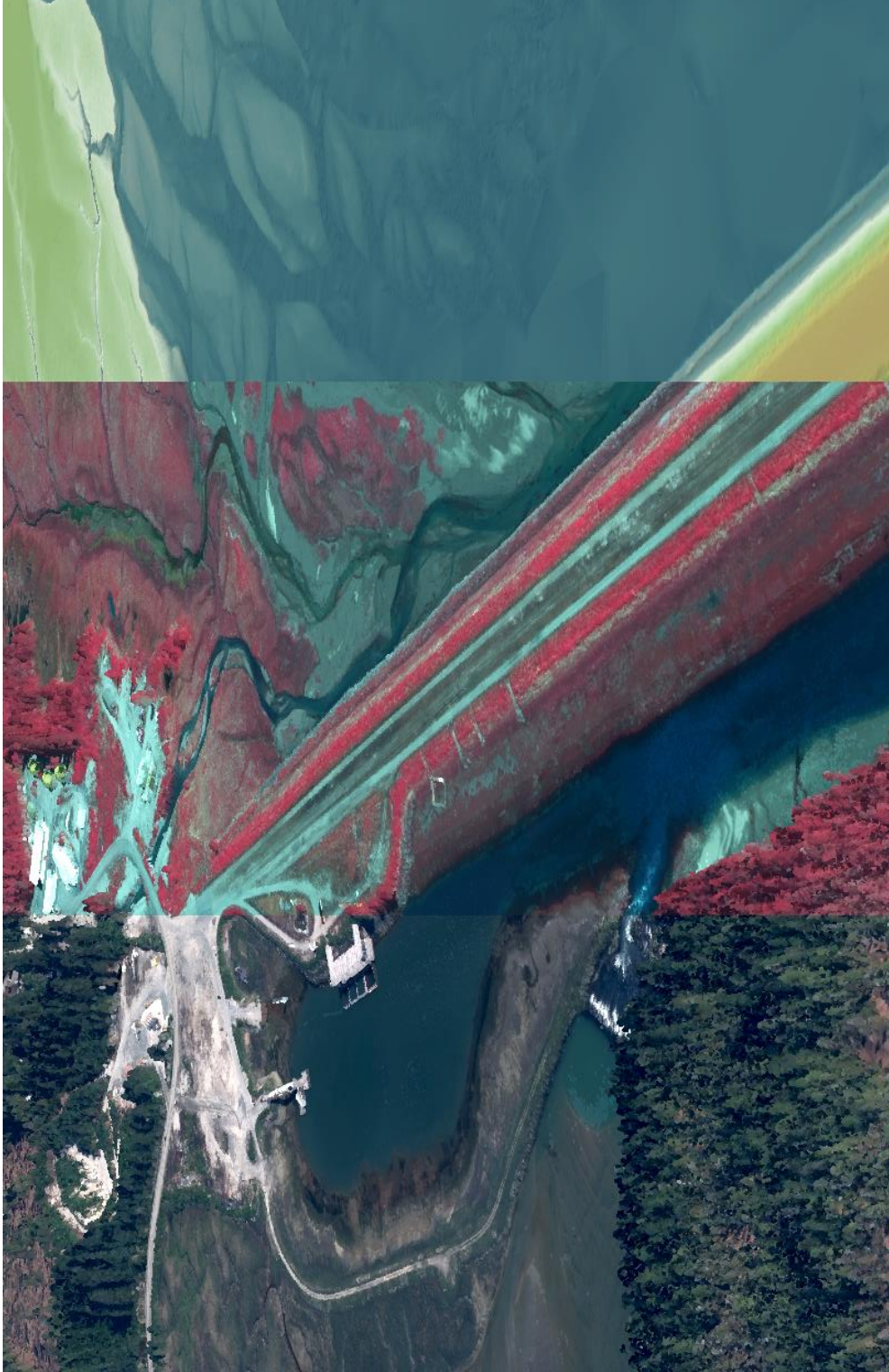


Figure 19: View looking North at Port Snettisham. The image was created from gridded ground-classified LiDAR points colored by elevation (right), LiDAR point cloud colored by NIR imagery (middle), and 4-band orthoimagery (left), and RGB imagery (right).

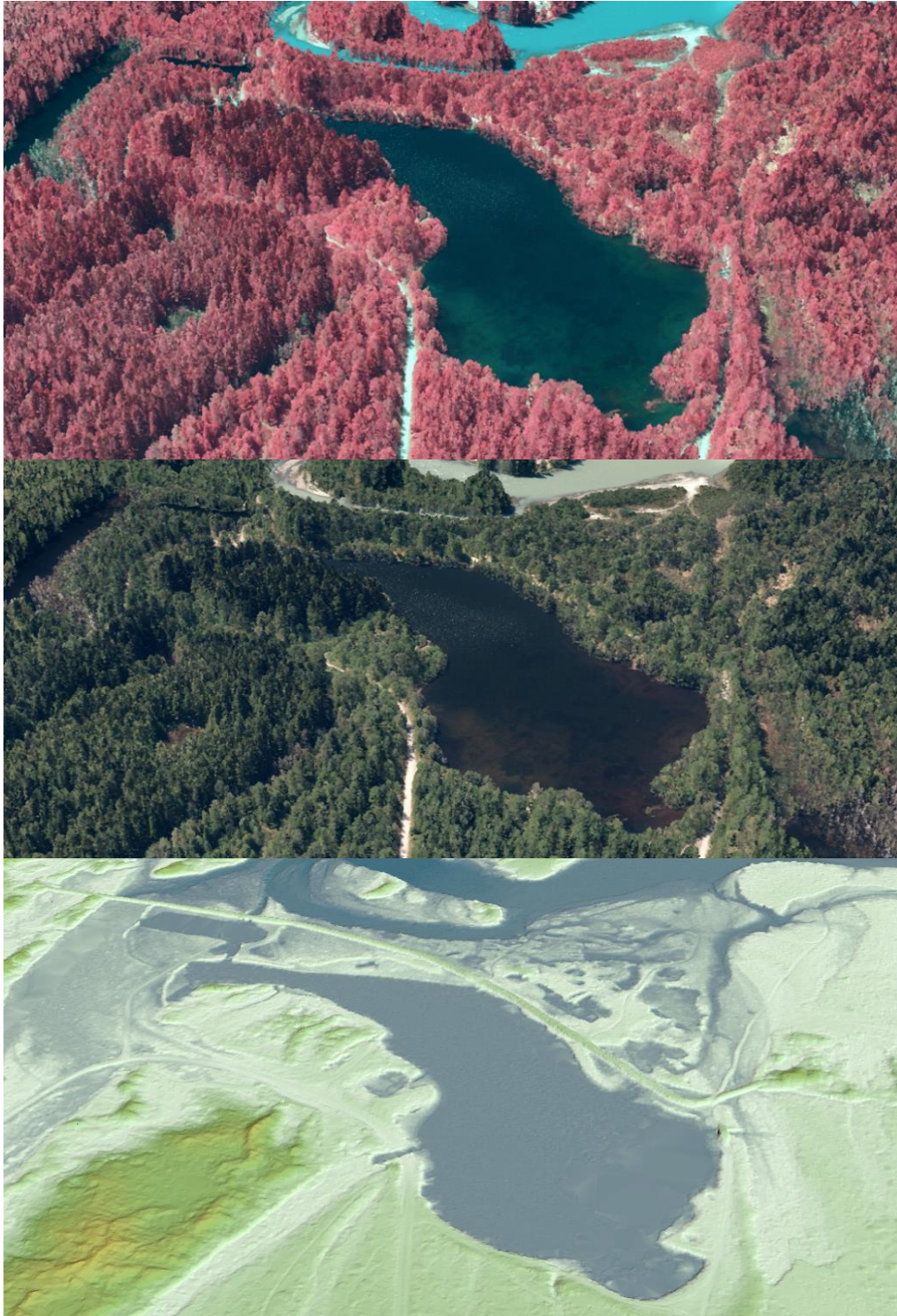


Figure 20: View looking west at small lakes and wetlands near Mendenhall Lake. The image was created from gridded ground-classified LiDAR points colored by elevation (bottom), LiDAR point cloud colored by 4-band orthoimagery (center) and NIR imagery (top).



Figure 21: View looking east over Back Loop Juneau near Mendenhall Lake. The image was created from LiDAR point cloud colored by NIR imagery (left), gridded ground-classified LiDAR points colored by elevation (center), and RGB imagery (right).

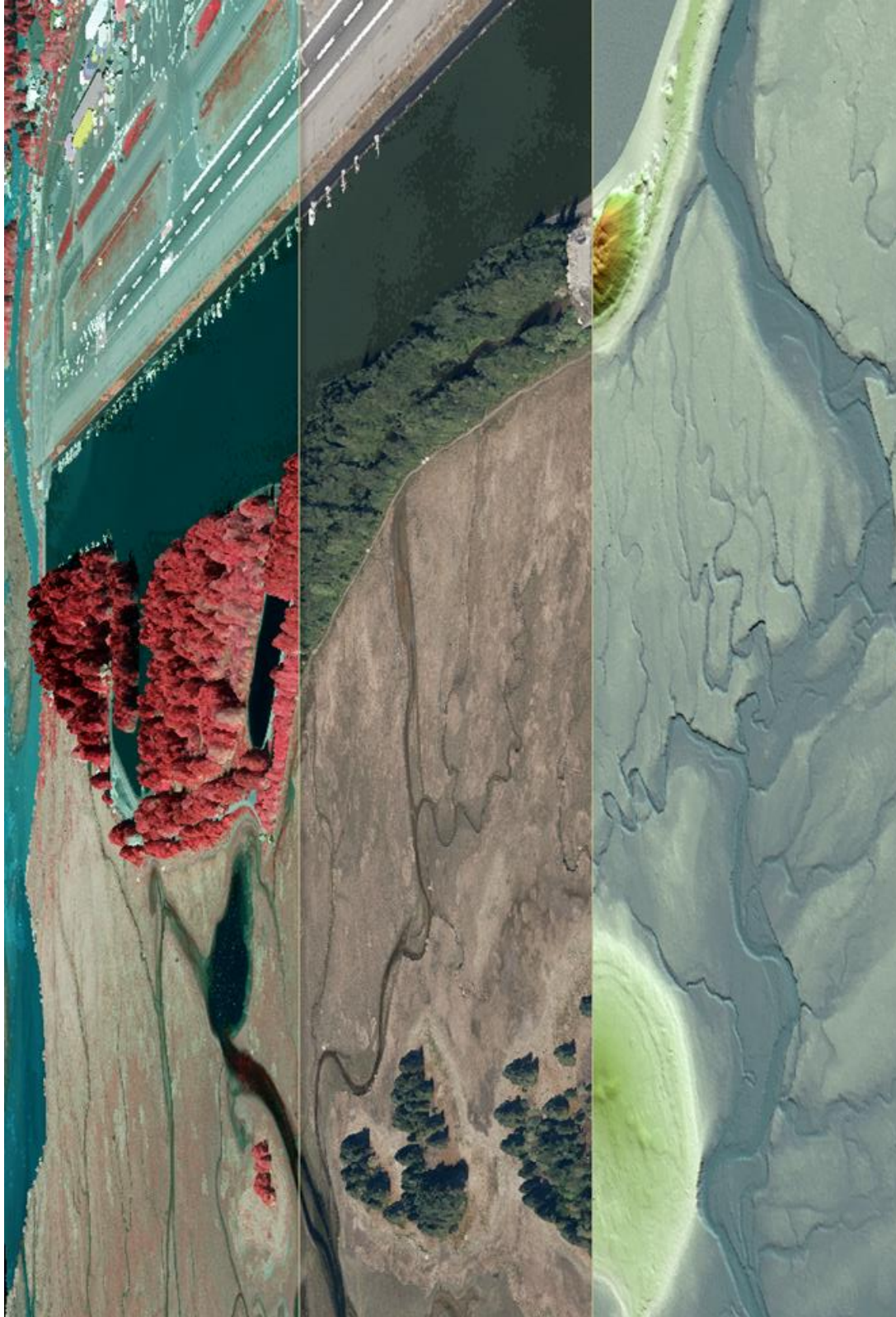


Figure 22: View looking northwest at the Mendenhall Wetland and the Juneau International Airport. The image was created from gridded ground-classified LiDAR points colored by elevation (bottom), LiDAR point cloud colored by 4-band orthoimagery (middle) and NIR imagery (top) orthoimagery.



R&M ENGINEERING, INC.
ENGINEERS
GEOLOGISTS
SURVEYORS

6205 GLACIER HWY. «» JUNEAU, ALASKA 99801
PHONE: 907-780-6060 «» FAX: 907-780-4611
EMAIL: rmengineering@rmjuneau.com

July 16, 2013

WSI LIDAR Quality Control Report

R & M Engineering, Inc. was contracted by WSI to conduct quality control and various verification measurements for LIDAR production conducted in the Juneau, Alaska area for 2013.

Utilizing R & M's established local GPS (Global Positioning System) network expanded as required to encompass the area of interest both existing and newly established monument positions were observed independently and apart from WSI observations. A summary of basis for position reporting follows:

- a.) Monuments coordinates are based on N.A.D. 1983, Alaska State Plane Coordinates, Epoch 2010.0000 for horizontal position.
- b.) Vertical datum utilized was NAVD 1988.

Each individual control station utilized for this project was observed through use of Trimble R8 II GPS receivers. Observation logs were completed for each station and observation period. A minimum of 120 minutes observation was accomplished at each control point. Each control network monument had a minimum of two observations periods ensuring adequate redundancy and self checks for the overall network.

Resulting observation data was processed through OPUS service utilizing NAD 1983 and GEOID 12A as the control basis. All network control points reported a 97% or better accuracy from the OPUS processing. Redundant horizontal positions at each control point were analyzed and then averaged prior to final position reporting. Where control points were located near established vertical control points (temporary bench marks and/or published bench mark stations) a closed spirit level circuit was conducted to compare differences between the reported OPUS processed orthometric elevations and known leveled elevations. The local bench mark elevation utilized is based on Mean Lower Low Water (M.L.L.W.) being 0.00 feet. The latest published elevation report through NOAA is dated 10/20/2011. These differences were then averaged and the resulting figure applied to all elevations in the following control verification report.



Mark A. Johnson, L.S.
Land Surveyor

Attachment: Ground Control Points

Serving Southeast Alaska For Over 44 Years

GCP

1,2363134.51,2489318.88,21.48,Outer
2,2495878.37,2449762.95,22.28,Echo
3,2347590.95,2559311.90,25.33,Thane
10,2363134.51,2489318.88,21.47,Outer
11,2394419.41,2479305.33,122.71,Juneau 01
12,2382075.10,2523642.96,25.00,Juneau 02
13,2347645.81,2559234.43,25.08,Juneau 03
14,2444262.21,2470844.82,31.52,Juneau 04
15,2354471.83,2522365.89,1133.68,Juneau 05
16,2362233.04,2541120.77,29.14,A14908
17,2383867.19,2507256.96,25.09,A14907
18,2491887.67,2446938.66,49.38,GPS 11
19,2478268.16,2444689.89,112.52,Tongass1
1000,2347645.79,2559234.42,25.15,JUNEAU-03
1001,2347663.88,2559240.39,26.52,PK-X
1002,2347688.44,2559230.54,27.54,PK-X
1003,2342505.94,2564622.69,107.55,WHITE PAINT STRIP
1004,2347812.44,2559090.37,29.06,.BRIDGE
1005,2347904.71,2558990.11,29.08,/BRIDGE
1006,2349185.76,2557981.69,62.21,.EP
1007,2349222.81,2557908.73,60.40,/EP
1008,2352386.40,2554165.46,77.31,GR
1009,2352536.17,2553989.71,64.60,PP
1010,2352636.05,2553896.39,59.37,GR
1011,2358201.85,2547692.51,61.95,WT STRIP
1012,2358114.12,2547784.85,57.16,WT STRIP
1013,2358060.46,2546494.42,49.76,.CROSSWALK
1014,2358027.32,2546467.75,49.15,/CROSSWALK
1015,2362334.51,2543723.75,27.36,.CROSSWALK
1016,2362337.58,2543748.95,27.01,/CROSSWALK
1017,2362325.02,2543768.58,27.04,.CROSSWALK
1018,2362307.68,2543786.05,27.44,/CROSSWALK
1019,2362341.44,2542200.08,26.08,.CROSSWALK
1020,2362330.92,2542147.67,26.63,/CROSSWALK
1021,2363030.70,2540168.52,27.21,.CROSSWALK
1022,2362996.95,2540195.30,26.89,/CROSSWALK
1023,2365832.60,2537249.98,25.64,PKW/X
1024,2372350.84,2532555.81,25.89,BUS ONLY ARROW
1025,2373416.61,2531098.63,33.38,ONLY ARROW
1026,2382044.26,2523570.95,24.91,mon lookout
1027,2382097.32,2523616.63,25.70,pkw/x
1028,2378899.27,2526697.69,55.96,ne cor arrow
1029,2378819.98,2526729.99,55.08,se cor arrow
1030,2380125.75,2527004.22,25.53,rm x
1031,2384182.32,2523002.79,29.68,cl east strip
1032,2384183.49,2522528.14,29.37,cl west strip
1033,2384451.99,2513175.96,26.36,wt/yelw ps
1034,2384162.53,2513745.59,26.73,ne wt/yelw ps
1035,2384747.96,2509882.74,26.92,.x-walk
1036,2384748.56,2509839.54,28.00,/x-walk
1037,2384604.68,2510018.88,27.00,.x-walk
1038,2384560.20,2510018.71,27.61,/x-walk
1039,2382044.25,2523571.00,24.93,check
1040,2444267.43,2470852.46,32.58,pk/washer
1041,2434763.99,2474629.17,29.74,cl paint strip
1042,2434812.24,2474656.00,30.06,cl paint strip
1043,2445132.54,2470372.67,36.22,pk/x
1044,2444885.05,2470508.67,33.17,wt strip
1045,2444957.94,2470464.94,33.81,wt strip
1046,2446484.71,2466218.98,25.66,arrow
1047,2446493.03,2466235.48,25.70,arrow
1048,2450354.77,2461589.61,45.79,pk/x
1049,2450545.35,2461390.56,39.84,end yellow strip

GCP
1050,2496022.91,2449651.91,19.44,clramp
1051,2496020.07,2449694.00,22.67,clramp
1052,2495640.95,2450521.42,94.71,end yellow cl
1053,2495628.19,2450513.38,94.39,end wt stripe
1054,2495669.57,2450525.25,95.94,end wt stripe
1056,2492551.20,2448813.10,59.69,cl yellow
1057,2492341.32,2448190.83,56.48,cl yellow

APPENDIX A – MLLW ADJUSTMENT

R&M Engineering, Inc. (Mark A. Johnson - AKPLS#7570) provided Mean Lower Low Water (MLLW) elevations for each monument used in this project. These MLLW elevations were determined by running level loops from tidal benchmarks with published MLLW elevations to each monument. Differences between the orthometric elevation of each monument on GEOID2012A and the MLLW elevation are shown in the table below, in meters.

PID	Ortho GEOID12A	Ortho MLLW	Difference
AI4907	6.576	7.647	1.071
AI4908	7.751	8.882	1.131
GPS_11	14.072	15.051	0.979
JUNEAU_01	36.354	37.402	1.048
JUNEAU_02	6.533	7.620	1.087
JUNEAU_03	6.585	7.644	1.059
JUNEAU_04	8.633	9.607	0.974
JUNEAU_05	344.432	345.546	1.114
TONGASS_01	33.356	34.296	0.940

The average MLLW adjustment was approximately 1.045m with a standard deviation of 0.066m. The ellipsoidal MLLW elevations shown in Table 3 were determined by adjusting the Ortho MLLW elevations shown above from GEOID2012A to the ellipsoid. As a result of being calibrated using the ellipsoidal MLLW elevations instead of the normal ellipsoidal elevations, the LiDAR data was adjusted to the MLLW vertical datum.

1-sigma (σ) Absolute Deviation: Value for which the data are within one standard deviation (approximately 68th percentile) of a normally distributed data set.

1.96-sigma (σ) Absolute Deviation: Value for which the data are within two standard deviations (approximately 95th percentile) of a normally distributed data set.

Accuracy: The statistical comparison between known (surveyed) points and laser points, typically measured as the standard deviation (σ) and root mean square error (RMSE).

Fundamental Vertical Accuracy (FVA):

Consolidated Vertical Accuracy (CVA):

Absolute Accuracy: The vertical accuracy of LiDAR data is described as the mean and standard deviation (σ) of divergence of LiDAR point coordinates from RTK ground survey point coordinates. To provide a sense of the model predictive power of the dataset, the root mean square error (RMSE) for vertical accuracy is also provided. These statistics assume the error distributions for x, y, and z are normally distributed, thus we also consider the skew and kurtosis of distributions when evaluating error statistics.

Relative Accuracy: Relative accuracy refers to the internal consistency of the data set - the ability to place a laser point in the same location over multiple flight lines, GPS conditions, and aircraft attitudes. Affected by system attitude offsets, scale, and GPS/IMU drift, internal consistency is measured as the divergence between points from different flight lines within an overlapping area. Divergence is most apparent when flight lines are opposing. When the LiDAR system is well calibrated, the line-to-line divergence is low (<10 cm).

Root Mean Square Error (RMSE): A statistic used to approximate the difference between real-world points and the LiDAR points. It is calculated by squaring all the values, then taking the average of the squares and taking the square root of the average.

Data Density: A common measure of LiDAR resolution, measured as points per square meter.

DTM / DEM: These often-interchanged terms refer to models made from laser points. The digital elevation model (DEM) refers to all surfaces, including bare ground and vegetation, while the digital terrain model (DTM) refers only to those points classified as ground.

Intensity Values: The peak power ratio of the laser return to the emitted laser. It is a function of surface reflectivity.

Laser Noise: For any given target, laser noise is the breadth of the data cloud per laser return (i.e., last, first, etc.). Lower intensity surfaces (roads, rooftops, still/calm water) experience higher laser noise.

Nadir: A single point or locus of points on the surface of the earth directly below a sensor as it progresses along its flight line.

Overlap: The area shared between flight lines, typically measured in percent; 100% overlap is essential to ensure complete coverage and reduce laser shadows.

Pulse Rate (PR): The rate at which laser pulses are emitted from the sensor; typically measured as thousands of pulses per second (kHz).

Pulse Returns: For every laser pulse emitted, the Leica ALS 60 system can record *up to four* wave forms reflected back to the sensor. Portions of the wave form that return earliest are the highest element in multi-tiered surfaces such as vegetation. Portions of the wave form that return last are the lowest element in multi-tiered surfaces.

Real-Time Kinematic (RTK) Survey: GPS surveying is conducted with a GPS base station deployed over a known monument with a radio connection to a GPS rover. Both the base station and rover receive differential GPS data and the baseline correction is solved between the two. This type of ground survey is accurate to 1.5 cm or less.

Scan Angle: The angle from nadir to the edge of the scan, measured in degrees. Laser point accuracy typically decreases as scan angles increase.

Spot Spacing: Also a measure of LiDAR resolution, measured as the average distance between laser points.

APPENDIX C - ACCURACY CONTROLS

Relative Accuracy Calibration Methodology:

Manual System Calibration: Calibration procedures for each mission require solving geometric relationships that relate measured swath-to-swath deviations to misalignments of system attitude parameters. Corrected scale, pitch, roll and heading offsets were calculated and applied to resolve misalignments. The raw divergence between lines was computed after the manual calibration was completed and reported for each survey area.

Automated Attitude Calibration: All data were tested and calibrated using TerraMatch automated sampling routines. Ground points were classified for each individual flight line and used for line-to-line testing. System misalignment offsets (pitch, roll and heading) and scale were solved for each individual mission and applied to respective mission datasets. The data from each mission were then blended when imported together to form the entire area of interest.

Automated Z Calibration: Ground points per line were used to calculate the vertical divergence between lines caused by vertical GPS drift. Automated Z calibration was the final step employed for relative accuracy calibration.

LiDAR accuracy error sources and solutions:

Type of Error	Source	Post Processing Solution
GPS (Static/Kinematic)	Long Base Lines	None
	Poor Satellite Constellation	None
	Poor Antenna Visibility	Reduce Visibility Mask
Relative Accuracy	Poor System Calibration	Recalibrate IMU and sensor offsets/settings
	Inaccurate System	None
Laser Noise	Poor Laser Timing	None
	Poor Laser Reception	None
	Poor Laser Power	None
	Irregular Laser Shape	None

Operational measures taken to improve relative accuracy:

Low Flight Altitude: Terrain following is employed to maintain a constant above ground level (AGL). Laser horizontal errors are a function of flight altitude above ground (i.e., $\sim 1/3000^{\text{th}}$ AGL flight altitude).

Focus Laser Power at narrow beam footprint: A laser return must be received by the system above a power threshold to accurately record a measurement. The strength of the laser return is a function of laser emission power, laser footprint, flight altitude and the reflectivity of the target. While surface reflectivity cannot be controlled, laser power can be increased and low flight altitudes can be maintained.

Reduced Scan Angle: Edge-of-scan data can become inaccurate. The scan angle was reduced to a maximum of $\pm 15^\circ$ from nadir, creating a narrow swath width and greatly reducing laser shadows from trees and buildings.

Quality GPS: Flights took place during optimal GPS conditions (e.g., 6 or more satellites and PDOP [Position Dilution of Precision] less than 3.0). Before each flight, the PDOP was determined for the survey day. During all flight times, a dual frequency DGPS base station recording at 1-second epochs was utilized and a maximum baseline length between the aircraft and the control points was less than 19 km (11.5 miles) at all times.

Ground Survey: Ground survey point accuracy (i.e. <1.5 cm RMSE) occurs during optimal PDOP ranges and targets a minimal baseline distance of 4 miles between GPS rover and base. Robust statistics are, in part, a function of sample size (n) and distribution. Ground survey RTK points are distributed to the extent possible throughout multiple flight lines and across the survey area.

50% Side-Lap (100% Overlap): Overlapping areas are optimized for relative accuracy testing. Laser shadowing is minimized to help increase target acquisition from multiple scan angles. Ideally, with a 50% side-lap, the most nadir portion of one flight line coincides with the edge (least nadir) portion of overlapping flight lines. A minimum of 50% side-lap with terrain-followed acquisition prevents data gaps.

Opposing Flight Lines: All overlapping flight lines are opposing. Pitch, roll and heading errors are amplified by a factor of two relative to the adjacent flight line(s), making misalignments easier to detect and resolve.